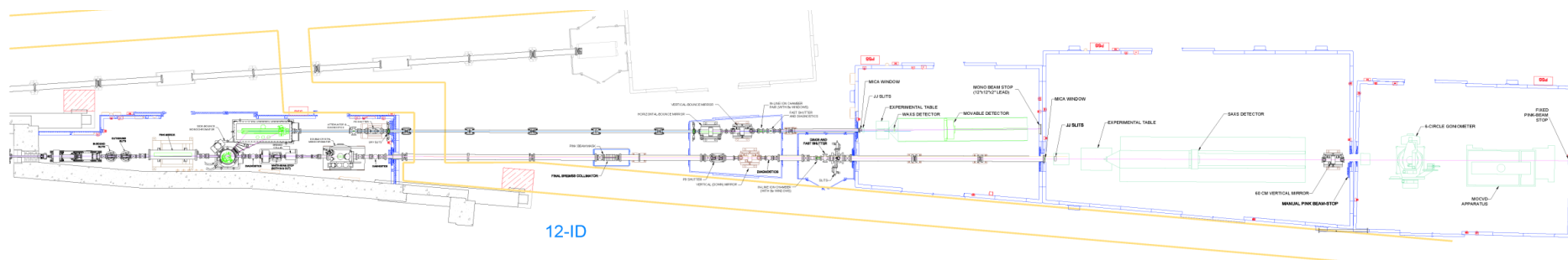




**Randall E. Winans and Sungsik Lee**  
**X-Ray Science Division**

**SAS Short Course**  
**“Beyond  $R_G$ ”**  
**Advanced Photon Source**  
**March 20, 2012**



**Work at APS Supported by the Office of Science, Basic Energy Sciences**

# Acknowledgements

## **CMS – XSD Group**

Byeongdu Lee  
Soenke Seifert  
Sungsik Lee (IACT)  
Tao Li (IACT)  
Robert Klingler

## **Institute Atom-efficient Chemical Transformations**



Justin Notestein (Northwestern U)  
Christian Canlas (Northwestern U)  
Kenneth Poepelmeier (Northwestern U)  
Linhua Hu (Northwestern U)  
Jeff Elam ES  
Chris Marshall CSE  
James Dumesic (Wisconsin)  
Brandon O'Neill (Wisconsin)

## **Materials Science Division**

Stefan Vajda  
Larry Curtis

## **Air Force MURI and BRI**

Juan Wang (CMS and U of Utah)  
Scott Anderson (U of Utah)  
Hai Wang (U Southern California)  
Jim Dumesic (U of Wisconsin)

## **Soot**

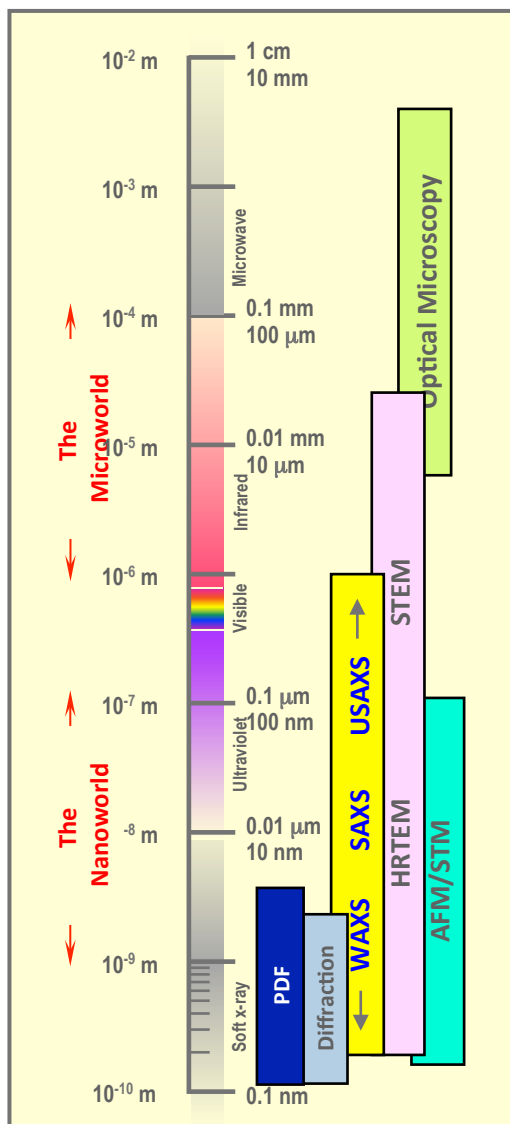
Jan Hessler (CSE)  
Rob Tranter (CSE)

## **CO<sub>2</sub> Sequestration**

Joseph Calo (Brown U)  
Jonathan Mathews (Penn State U)



# Synchrotron SAXS Methods for In Situ Studies



## 1. SAXS capabilities

- Access length scales 0.2 – 500 nm
- Particle size, shape, surface properties, porosity and element specific information from ASAXS
- Time resolution with pink beam
  - Ring timing – 3.7 microsec
  - Pump– probe -100 ps

## 2. In situ SAXS reactors

- High temperature oven for capillaries 600°C
- Very high temperature burners 1300°C
- Flow system, 0.8 mm cap. reactor 700°C

## 3. Grazing Incidence SAXS (GISAXS)

- Study particles and clusters on surfaces
- In situ
- All the information from regular SAXS plus height and width Information and more

# *Outline*

- 1. Catalytic combustion**
- 2. Particle formation in combustion**
- 3. CO<sub>2</sub> uptake in porous media**
- 4. Heterogeneous catalysis**





# *Understanding Catalytic Combustion Using SAXS and PDF*



International Workshop on Frontiers in Synchrotron Tools  
for Studies of Combustion and Energy Conversion

October 15 - 18, 2011    Shanghai, China

This work is supported by the Air Force Office of Scientific Research (AFOSR) Award:  
FA9550-08-1-0400.



# Catalytic Combustion for Propulsion

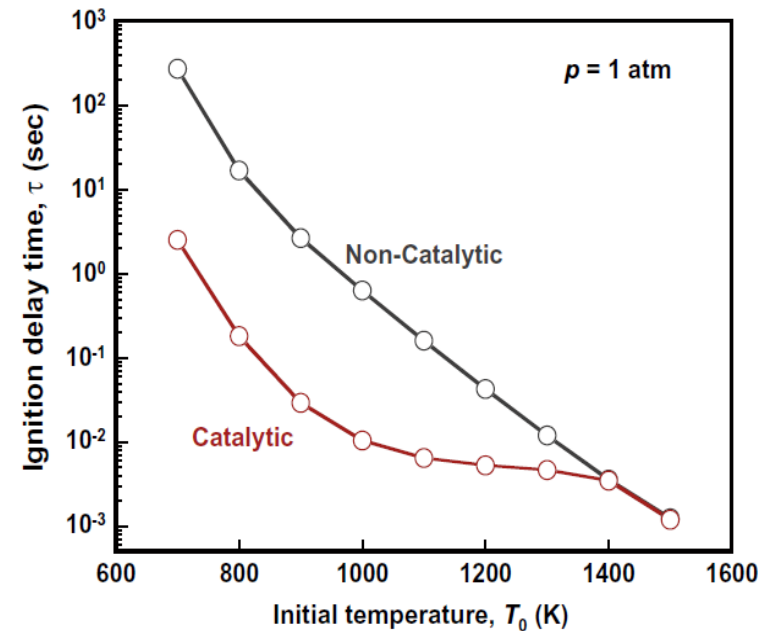
## Problem and Focus

- Traditional fixed bed supported catalyst will quickly be deactivated under propulsion conditions, which has led to development of fuel-soluble nanocatalysts.
- Insight is needed at many levels:
  - relationships between local catalyst structure
  - bonding and activity, support
  - surfactant effects on activity
  - mechanisms and changes in catalyst properties under propulsion conditions.



Use *in-situ* SAXS and PDF to study formation, growth and structure of catalyst nanoparticles which are produced from fuel-soluble precursors –

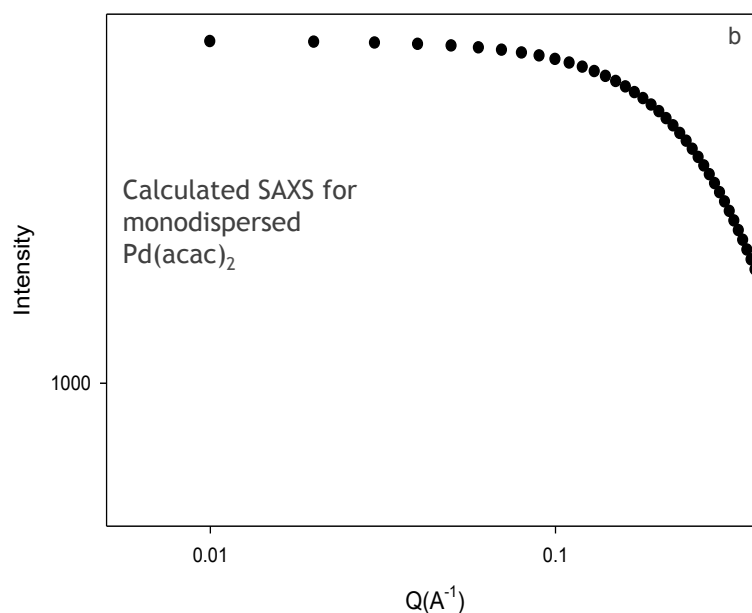
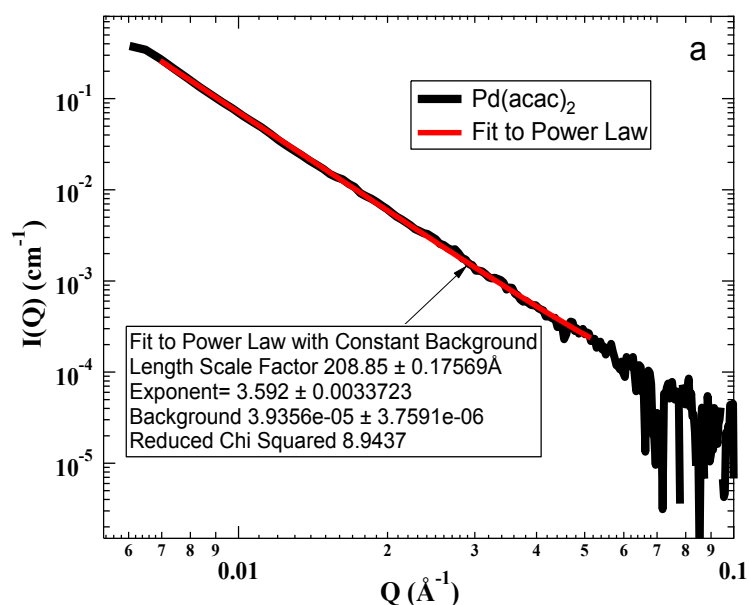
1. In the hot fuel
2. During combustion



T. Shimizu et al. Combust. Flame 97 (2010) 421

# SAXS Data from $\text{Pd}(\text{acac})_2$ in Toluene at 25 °C

Scattered intensity  $I(Q)$  versus scattering vector  $Q$ . The red line is the fit of a power law  $I(Q) \propto Q^{-D_f}$  with exponent  $D_f=3.6$

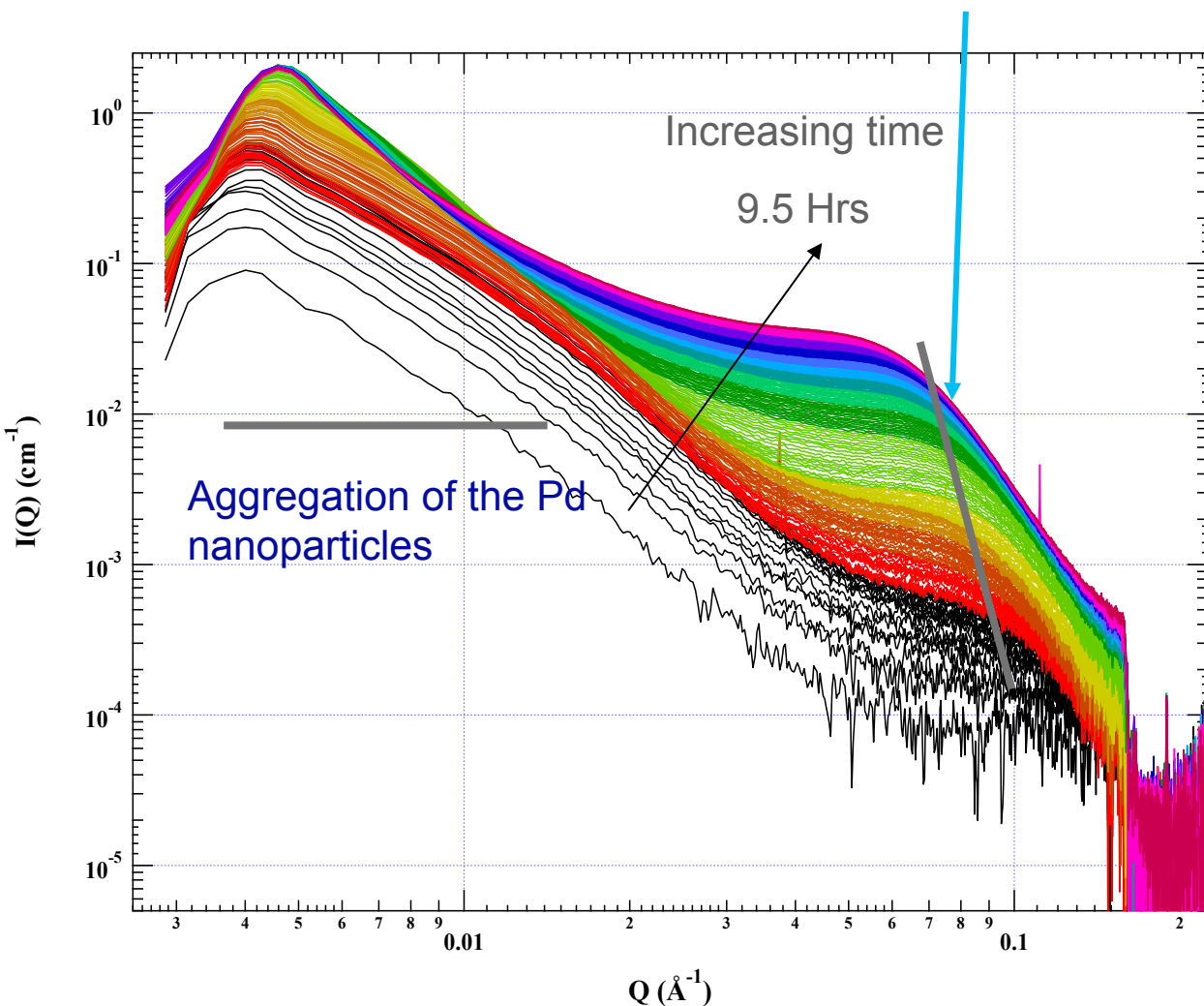


The  $D_f$  of 3.6 (exponent) suggests that there are large clusters with rough surfaces.

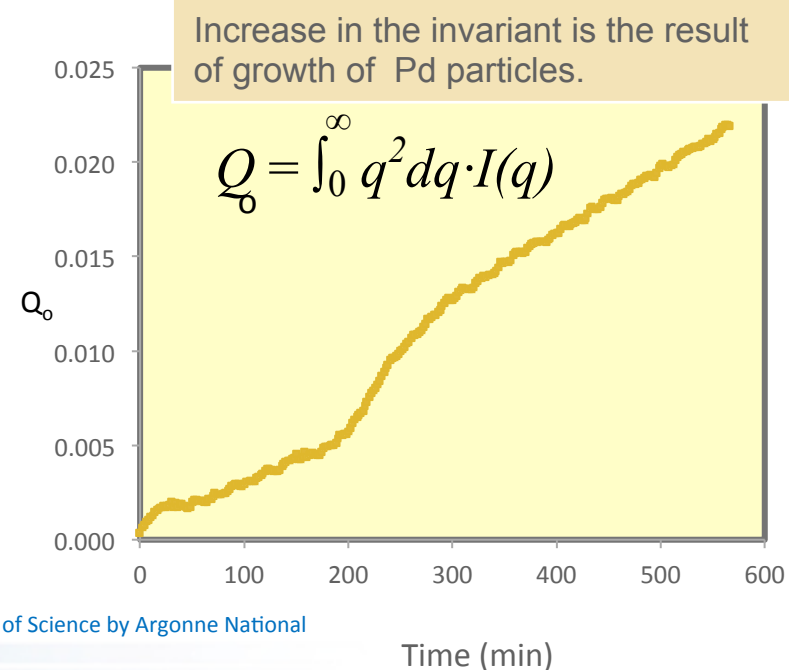
The lack of a Guinier region also suggests that the size of these clusters is polydispersed.

# Heating of Pd (acac)<sub>2</sub> in Toluene – Formation of Nanoparticles

Wang, Juan; Winans, Randall E.; Anderson, Scott Law; Seifert, Soenke; Lee, Byeongdu; Chupas, Peter Joseph; Ren, Yang; Lee, Sungsik; Liu, Yuzi, Journal of Physical Chemistry C (2013)



Broad peak which is moving slowly to lower  $Q$  range, which indicates that the particle size becomes larger

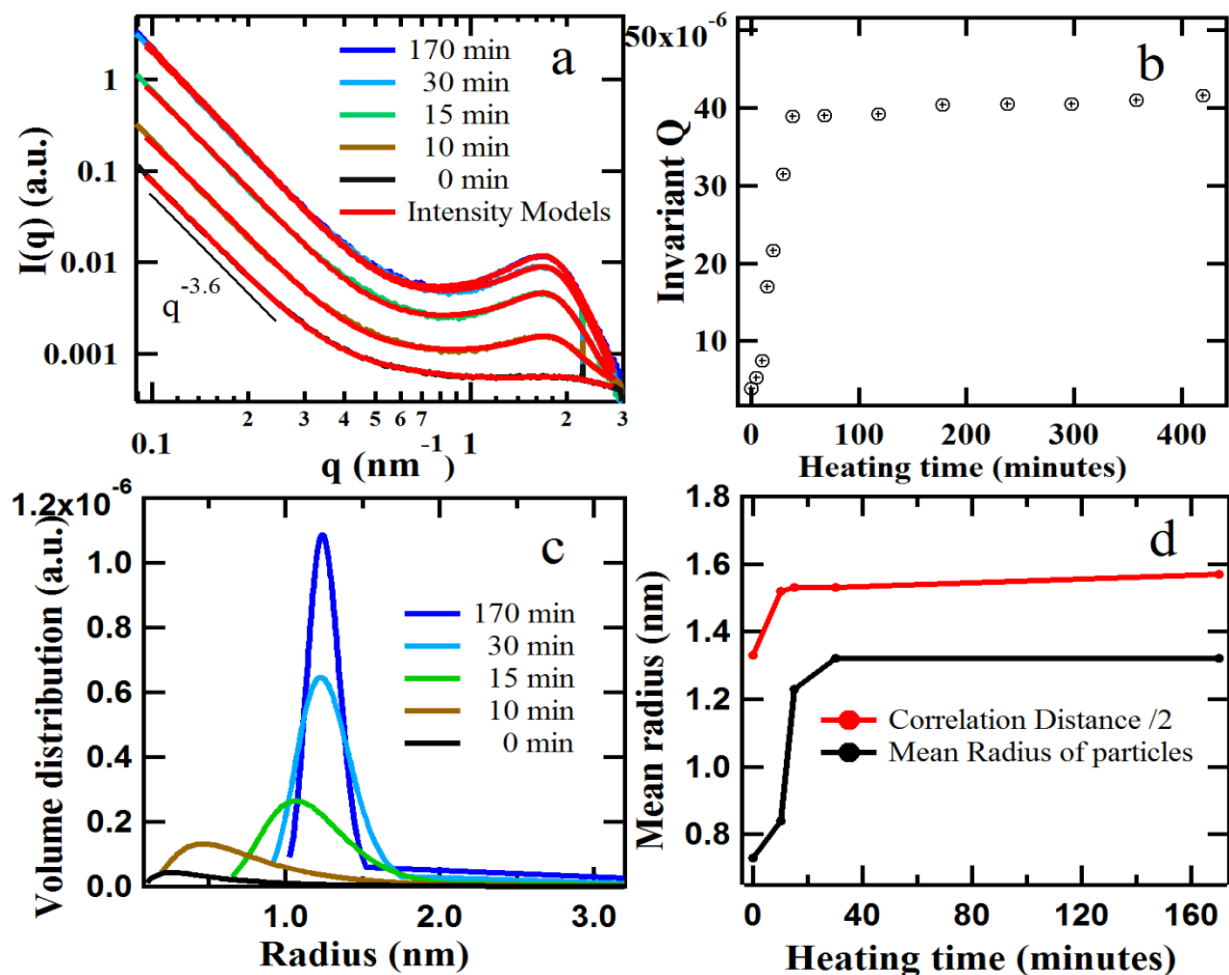


Scattering profiles from Pd nanoparticles measured every 2 minutes at 150 °C.

The Advanced Photon Source is an Office of Science User Facility operated for the U.S. Department of Energy Office of Science by Argonne National Laboratory

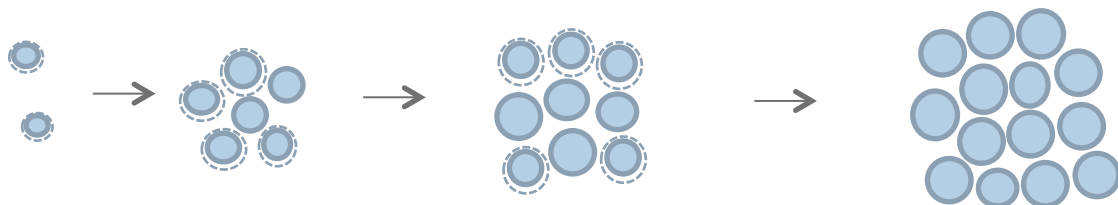
# *In situ SAXS for Pd(acetate)<sub>2</sub> – Solution Pd Particle Growth*

Changes with Time at 150 °C

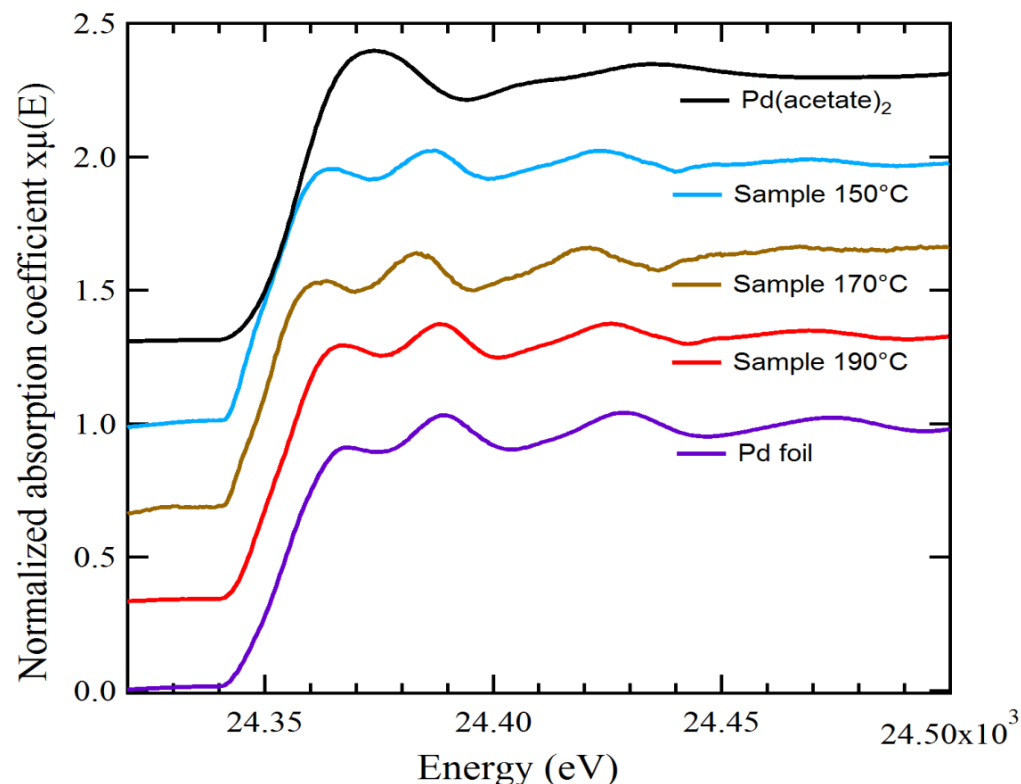


- Initial particle growth in the first 30 minutes.
- Correlation distance is larger than particle size which suggests that the particles are not close packed but capped with ligands.

Time (min)	Size (nm)
0	1.7
10	1.8
15	2.4
30	3.5
170	3.5



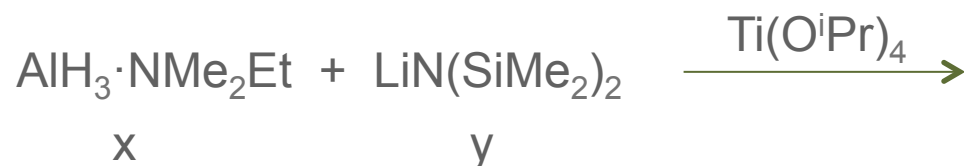
## *Pd K-edge XANES Spectra for Particles from Pd(acetate)<sub>2</sub> in Toluene*



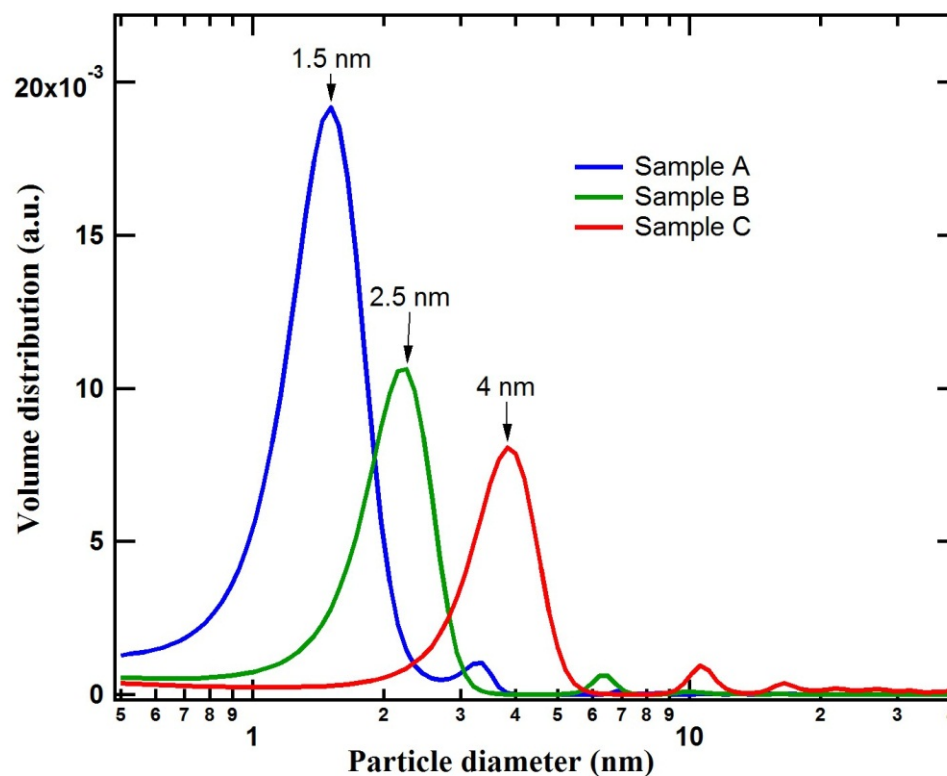
- Three samples heated at 150, 170 and 190 °C for 40 minutes, respectively.
- A feature at about 24.35 KeV reveals the appearance of the edge peak of Pd.
- The peak is broad at 150 °C, and become sharper and more similar to that of Pd foil with increasing temperature.
- This is in agreement with SAXS result that particles are capped with the ligands at low temperature, and at higher temperature the force between the particles and ligands is broken, so the spectrum of the sample at 190 °C is more similar to that of Pd foil.

# SAXS Size Analysis of Ligand Stabilized Al Nanoclusters

S. Mandel, J. Wang, R.E. Winans, L. Jessen, A. Sen, J. Phys. Chem. C, (2013) **117**, 6741.



x/y	Size (nm)
4	1.5
7	2.5
20	4.0

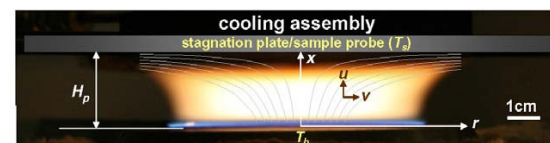
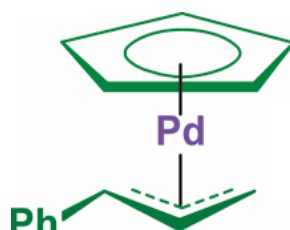




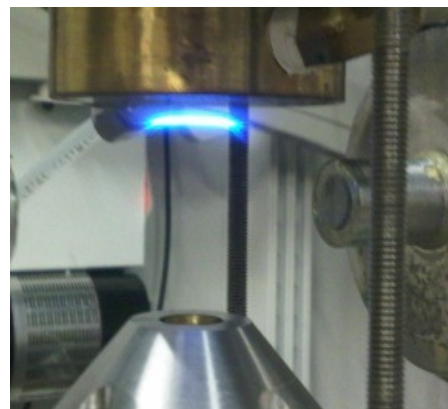
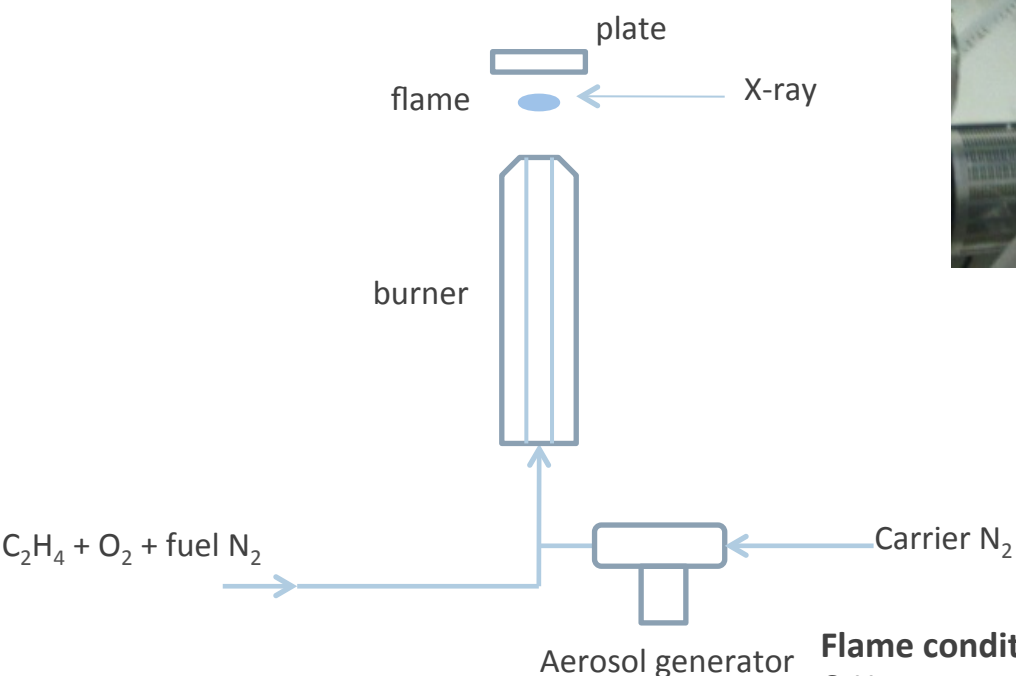
# SAXS Studies of Pd Particles in a Stagnation Burner Flame

Catalyst precursor:

$\text{Pd}(\eta^5\text{-C}_5\text{H}_5)(\eta^3\text{-1-PhC}_3\text{H}_4)$   
2.24 wt% ( $6.85\text{e-}5$  mol/L) in  
toluene



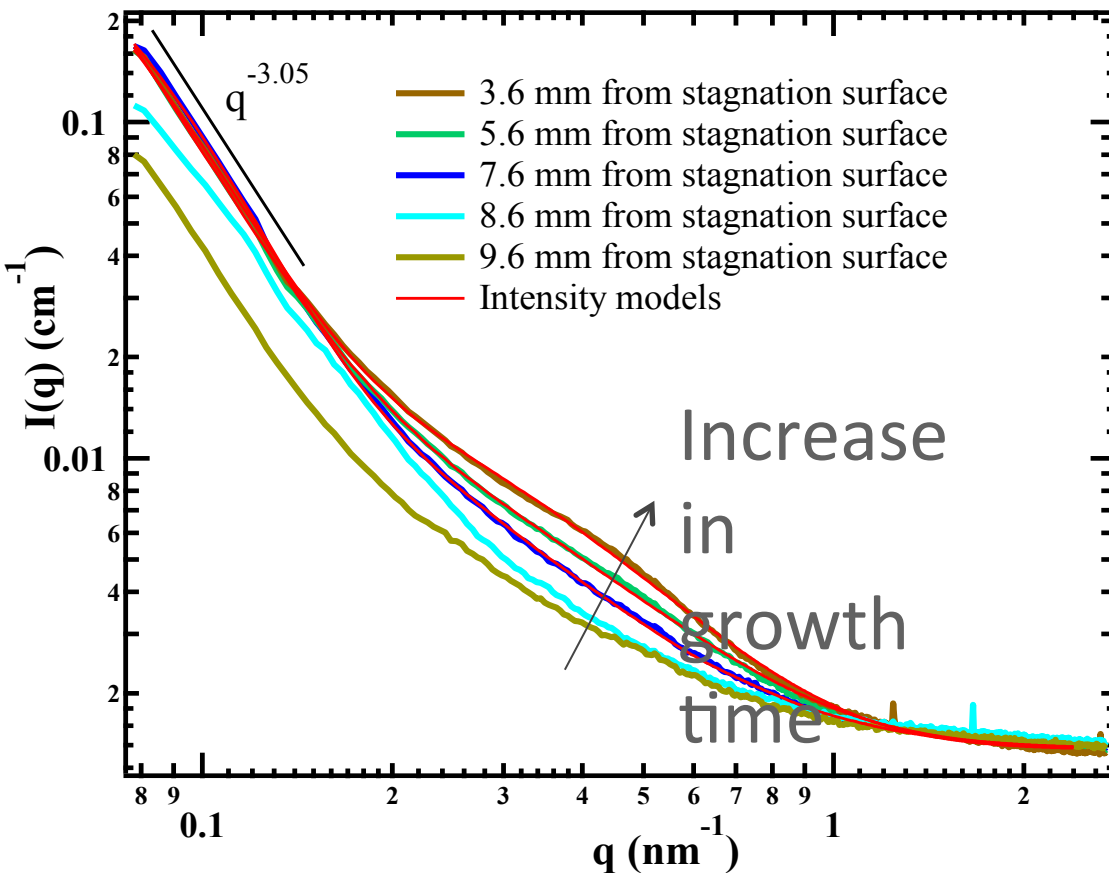
Aamir D. Abid, Joaquin Camacho, David A. Sheen, Hai Wang,  
Combustion and Flame 156 (2009) 1862–1870



## Flame conditions:

$\text{C}_2\text{H}_4$	0.31 L/min
$\text{O}_2$	1.34 L/min
Fuel $\text{N}_2$	3.40 L/min
$\text{N}_2$ coflow	2.97 L/min
Carrier $\text{N}_2$	125 mL/min

# Scattering Intensity At Several Distances from Stagnation Surface



SAXS intensity:

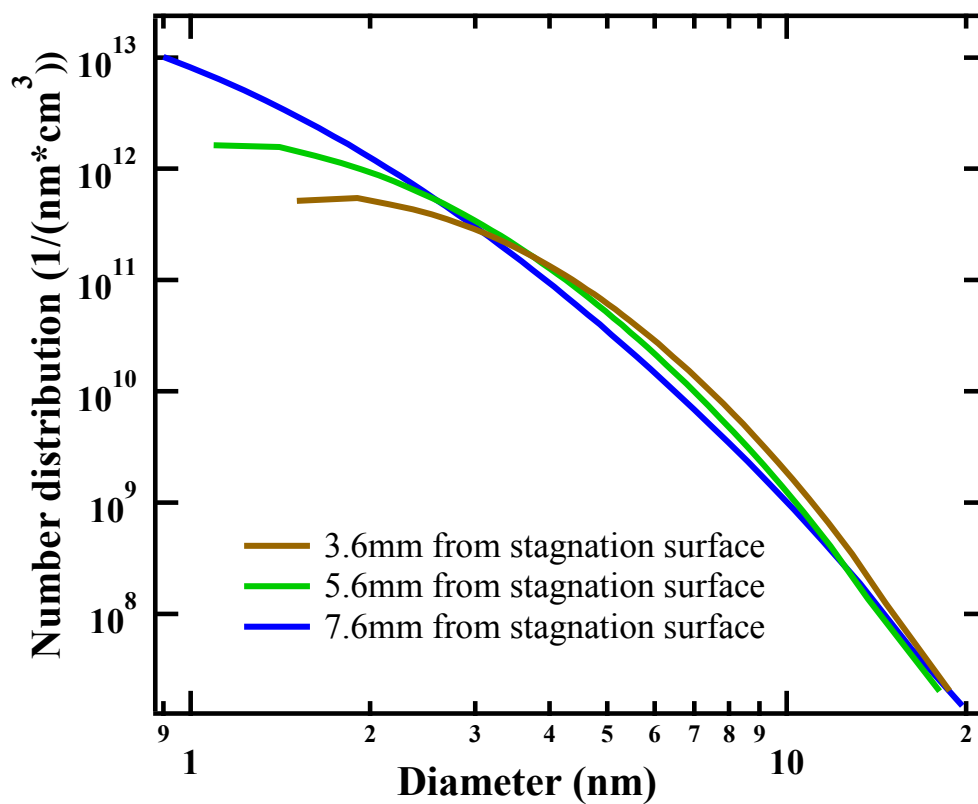
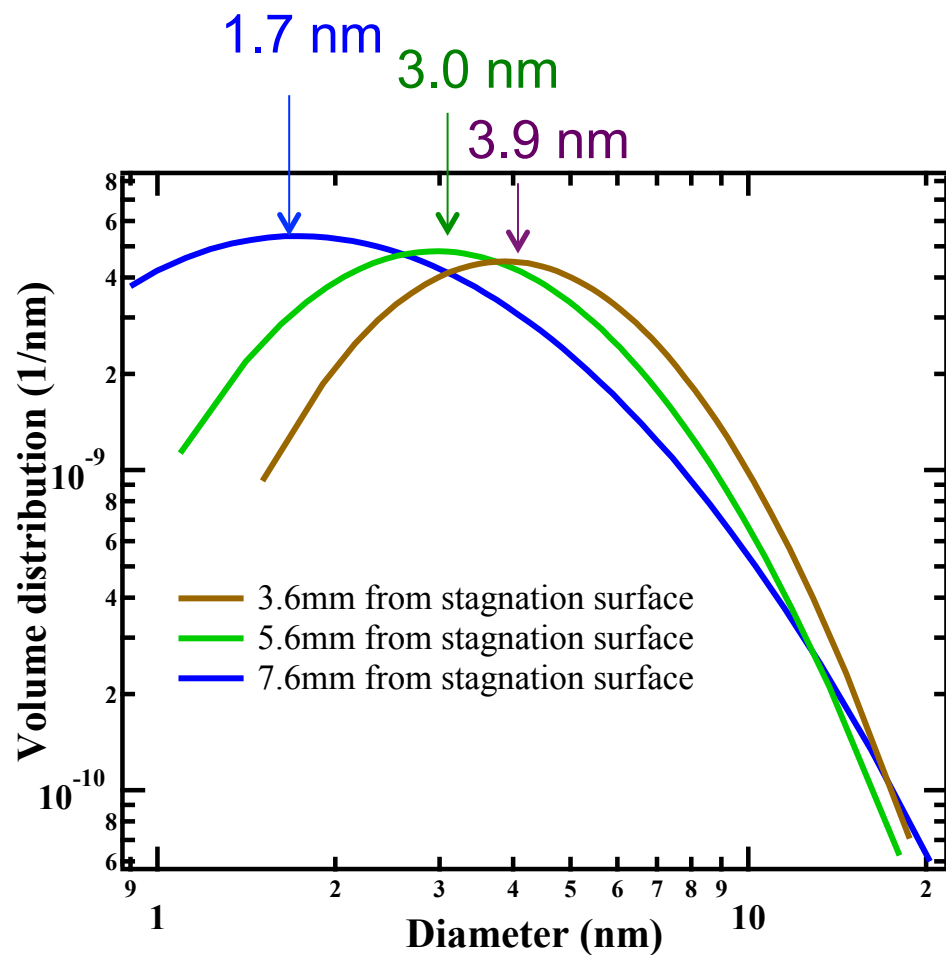
$$I(q) = N(\Delta\rho)^2 \left[ cq^{-D_f} + \bar{F}(q, \bar{r}) \right]$$

For polydispersed, spherical particles, the form factor is

$$\bar{F}(q, \bar{r}) = \int_0^{\bar{r}} V_p^2 \left[ \frac{3(\sin(qr) - qr \cos(qr))}{(qr)^3} \right]^2 P(r) dr$$

Ilavsky J.; Jemian, P. R. *J. Appl. Crystallogr.* **2009**, 42, 347-353.

# Size Distributions of the Primary Particles in Flame

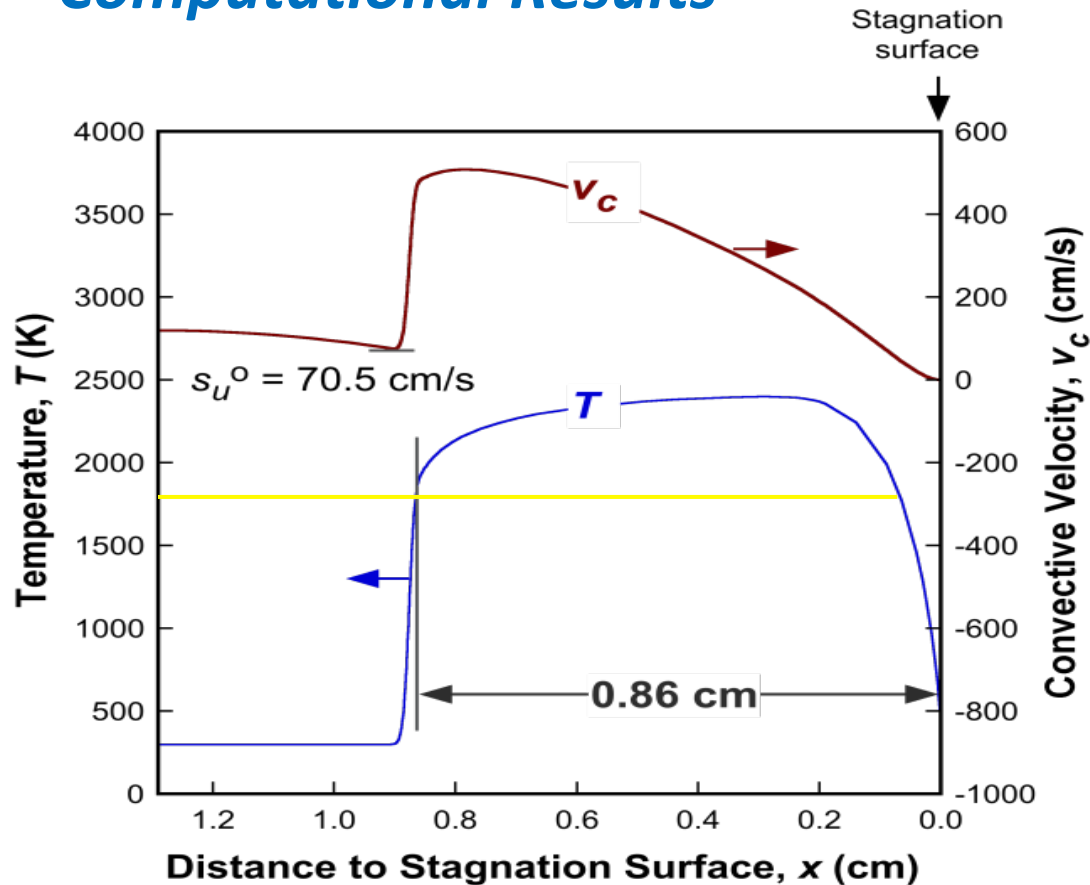


Volume Distribution

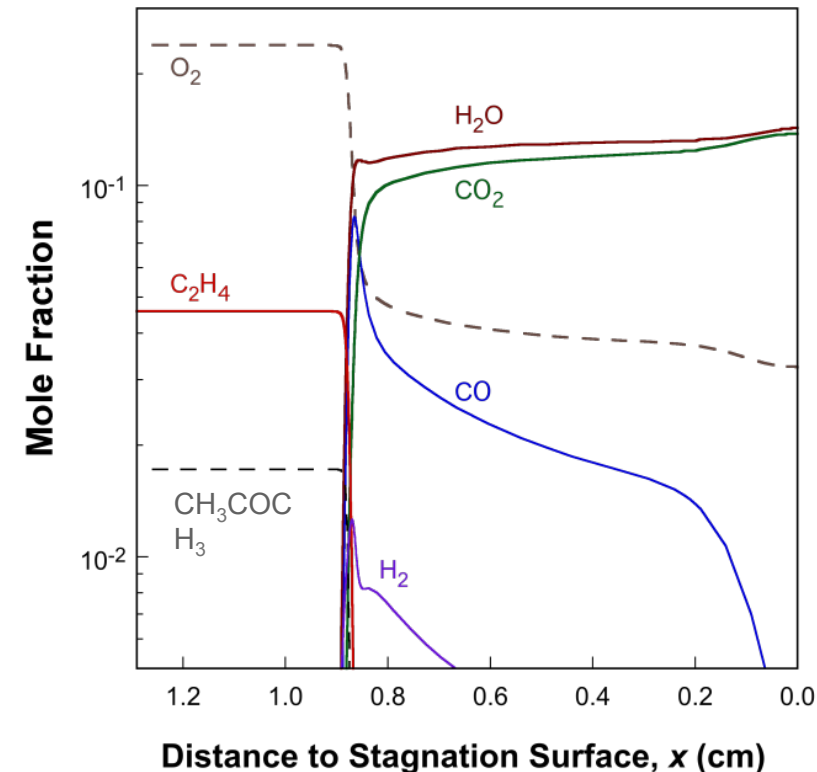
## Two Limiting Mechanisms

1. Aerosol drying followed by condensed-phase decomposition of  $\text{Pd}(\text{acetate})_2$  without fragmentation.
  - Droplet diameter  $\sim 3 \mu\text{m}$  @ 0.61 wt % of  $\text{Pd}(\text{acetate})_2$  loading produces Pd particles  $\sim 170 \text{ nm}$  in diameter, much larger than observed size.
2. Aerosol evaporation followed by gas-phase decomposition of  $\text{Pd}(\text{acetate})_2$  into a Pd vapor, followed by nucleation/growth into Pd particles.

# Computational Results

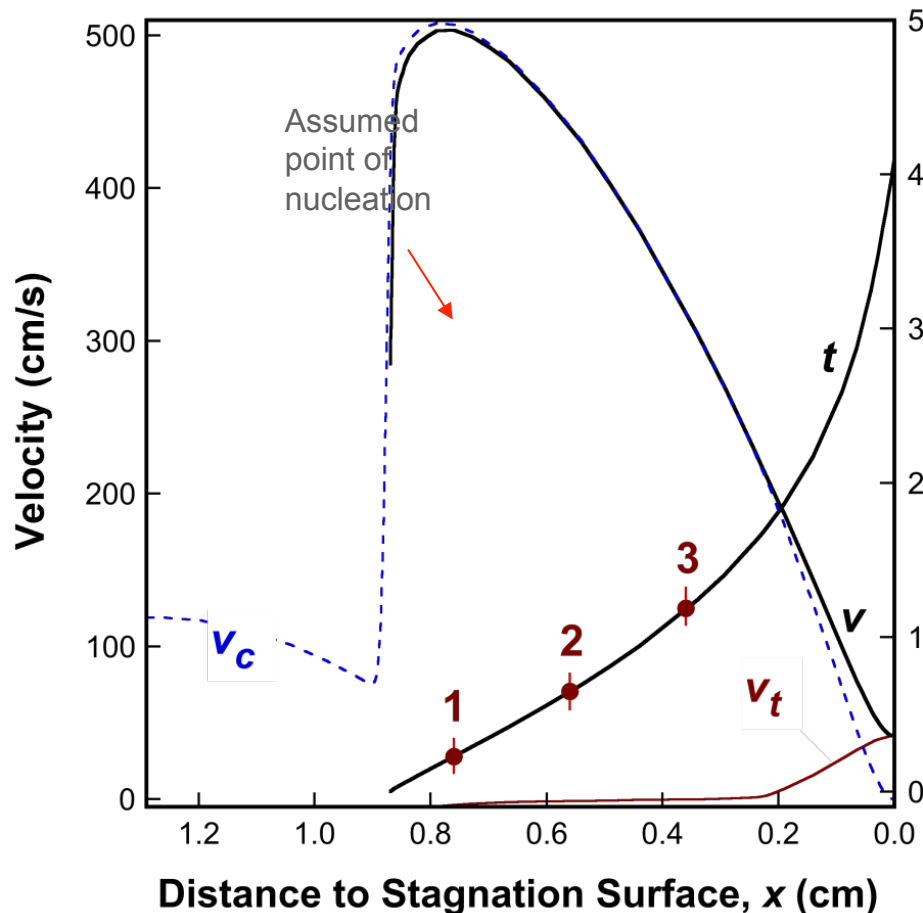


Major species profiles computed for the base flame.



- 1D flame modeling along the centerline of the stagnation flame using OPPDIF.
- Detailed reaction chemistry and transport (USC Mech II).
- Convective velocity ( $v_c$ ) and temperature ( $T$ ) calculated for the base flame with a stagnation temperature of 423 K.
- For a wide range of flame position, the gas  $T$  is higher than melting point of Pd (1828 K). The particles are expected to be molten until  $\sim 0.05$  cm from the stagnation surface.

# Computational Results



- Convective( $v_c$ ), thermophoretic( $v_t$ ) and total velocities( $v$ ) along the flame centerline and the particle residence time( $t$ ) in flames.

	$x$ (cm)	$t$ (ms)	$\langle D_p \rangle_v$ (nm)	
			Expt	Thero. Est.
1	0.76	0.23	1.7	2.1
2	0.56	0.65	3.0	2.9
3	0.36	1.19	3.9	3.6

Theoretical estimate used the 2<sup>nd</sup> order rate equation

$$N_t = N_o / (1 + \epsilon \beta N_o t)$$

The initial vapor density

$$N_o = 6.8 \times 10^{14} \text{ (#/cc)}$$

The collision kernel x van der Waals enhancement

$$\epsilon \beta = 2 \times 10^{-9} \text{ (cc/s)}$$

- The comparison suggest a vapor phase nucleation mechanism. A more accurate theoretical estimate requires the solution of master equations of collision.



## Conclusions

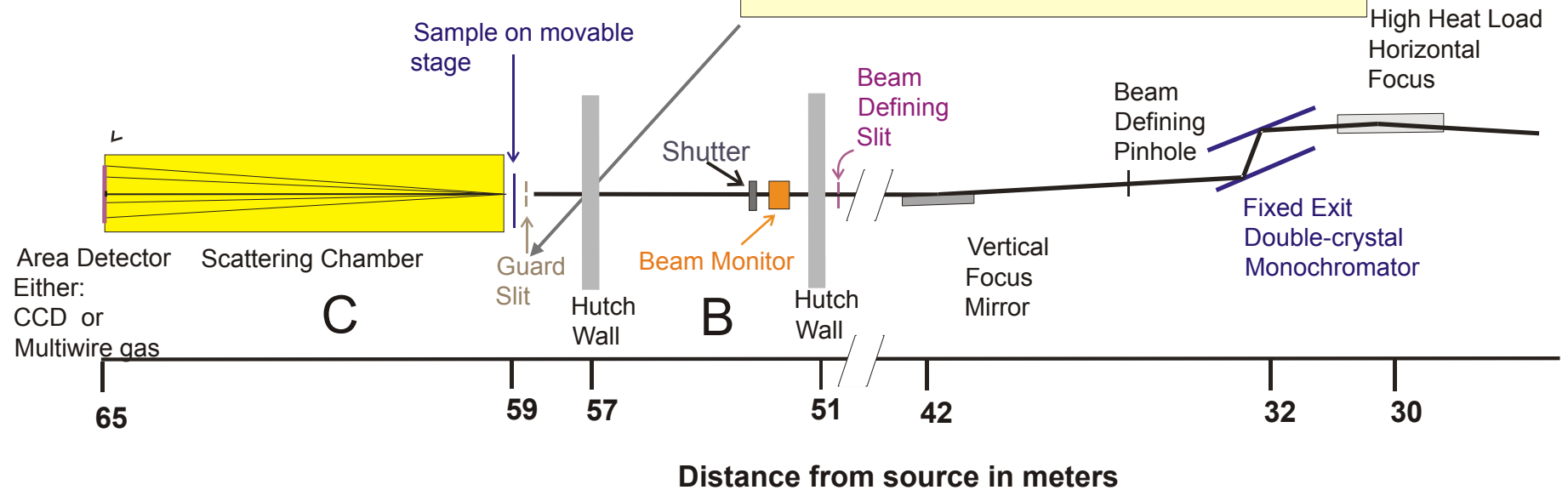
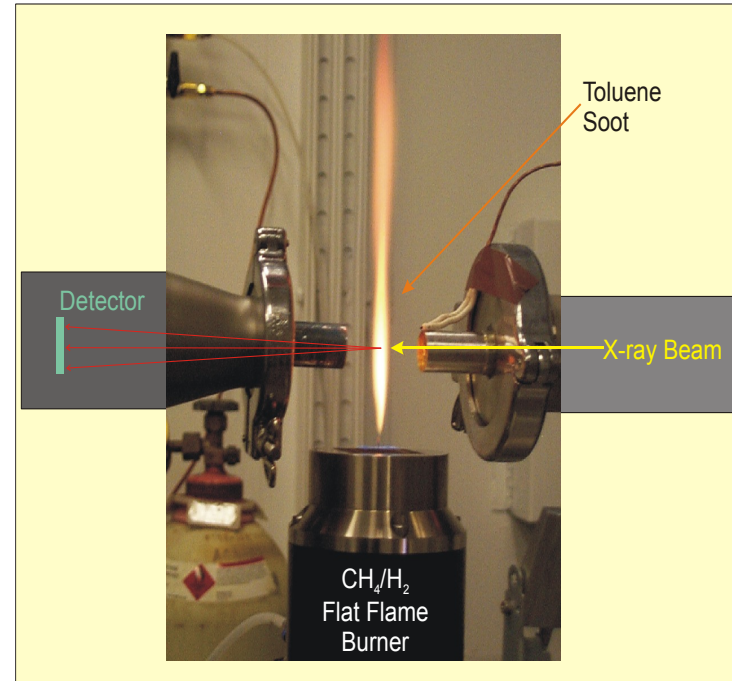
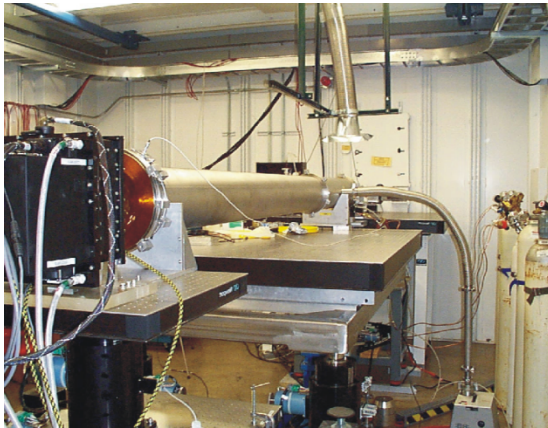
- Growth of Pd nanoparticles can be followed in solution with SAXS and PDF.
- The particles formed in solution are proved to be Pd.
- Particles appear to be produced from nucleation/growth of Pd vapor.



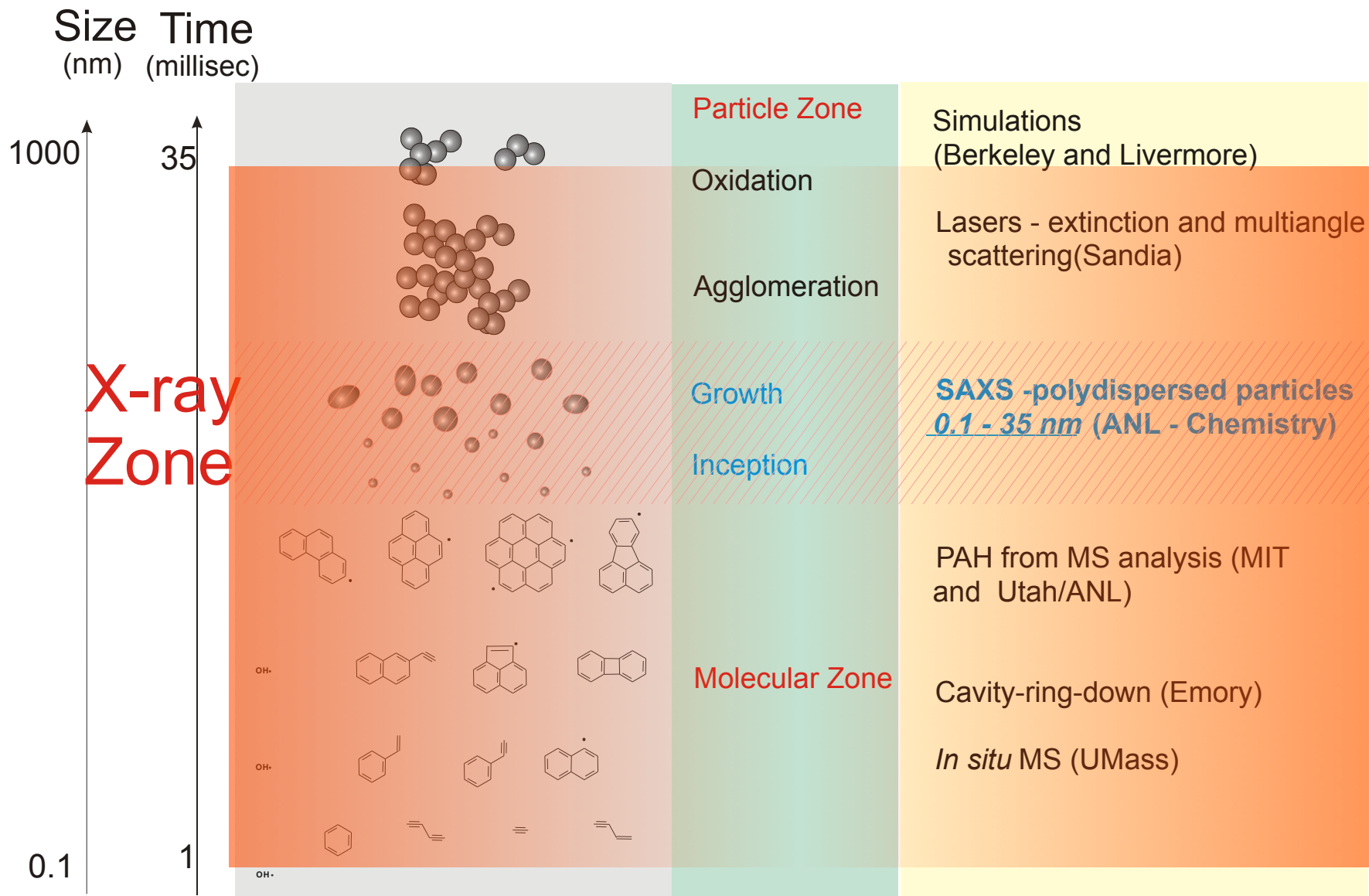


# Soot Formation Studies

## APS 12-ID-C Undulator Beamline

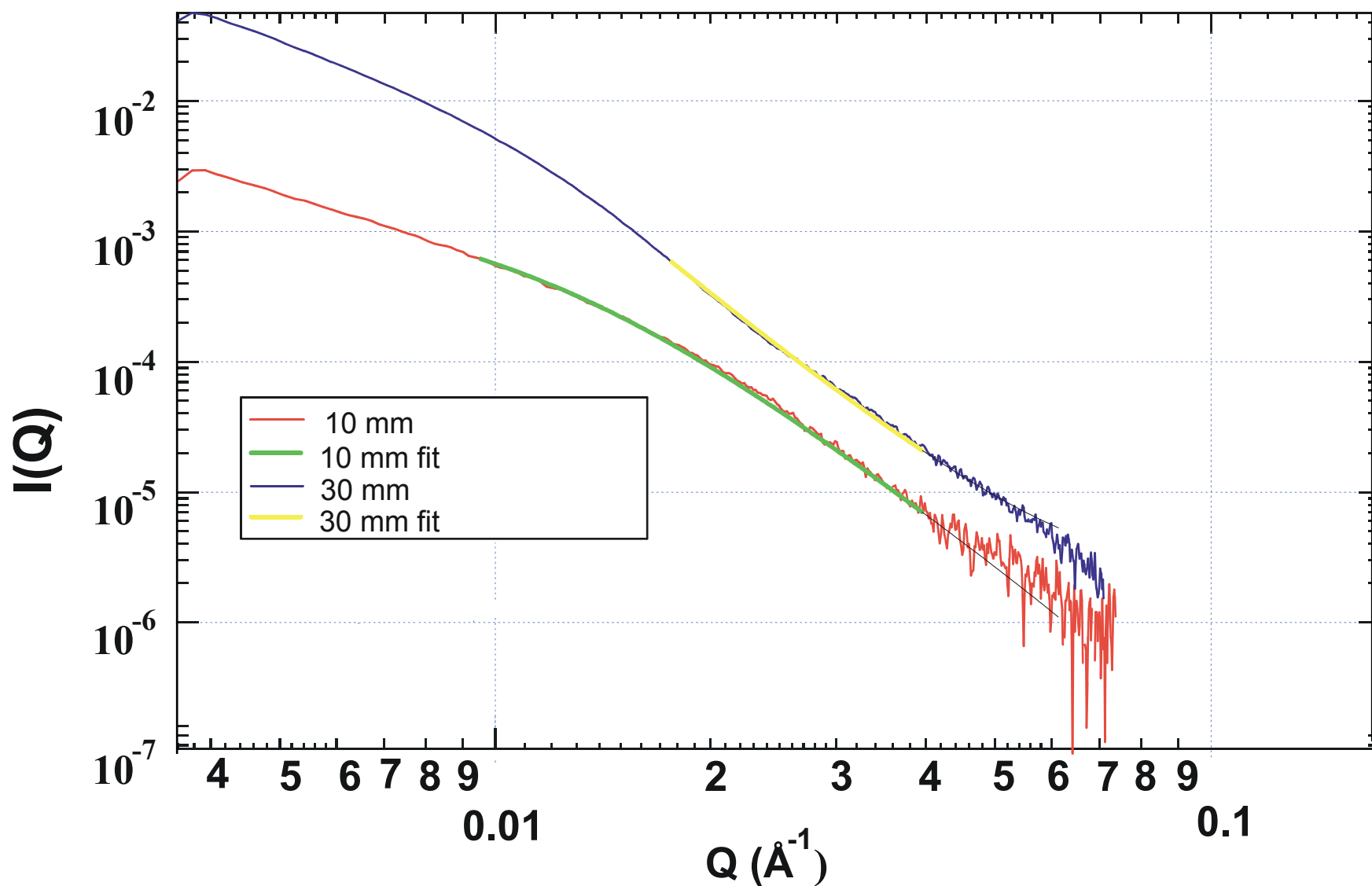


# Soot Formation



Hessler, Jan P.; Seifert, Soenke; Winans, Randall E.; Fletcher, Thomas H. Small-angle X-ray studies of soot inception and growth. Faraday Discussions (2001), 119(Combustion Chemistry: Elementary Reactions to Macroscopic Processes), 395-407.

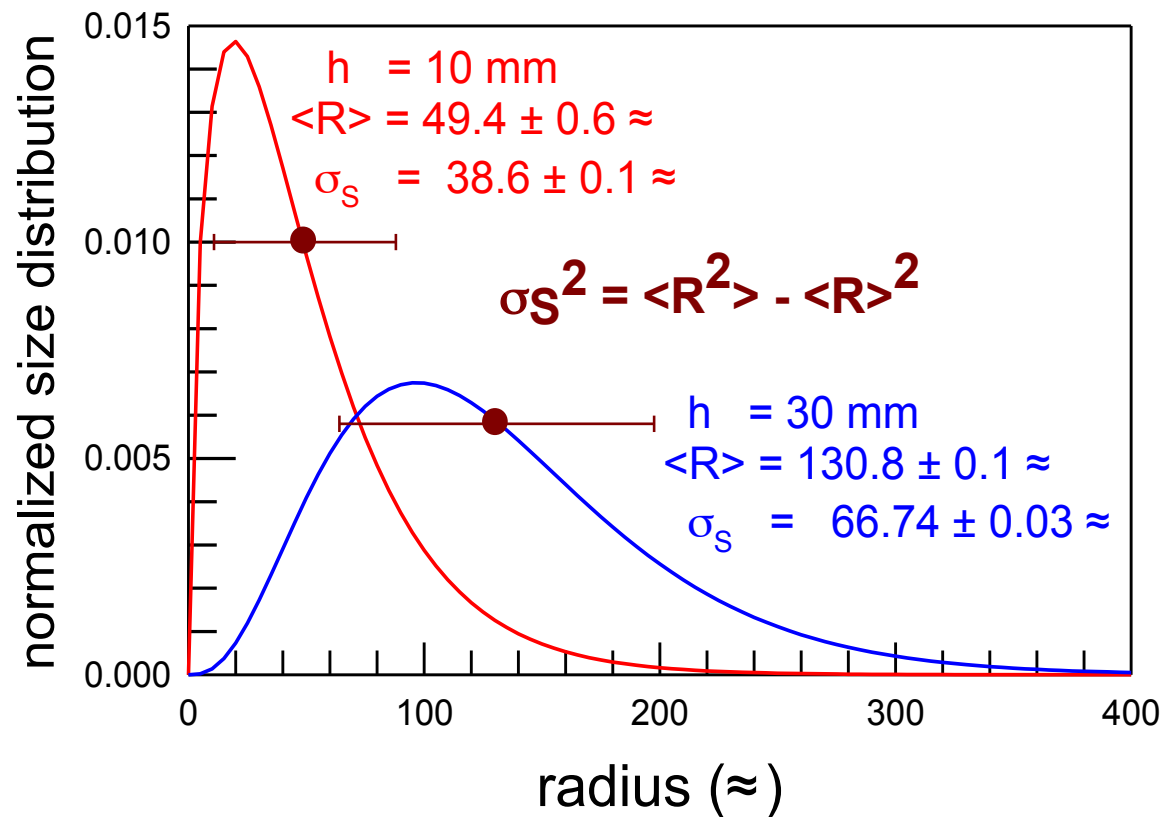
## SAXS Results for Soot from Toluene



Fit to Schultz polydispersed sphere form factor

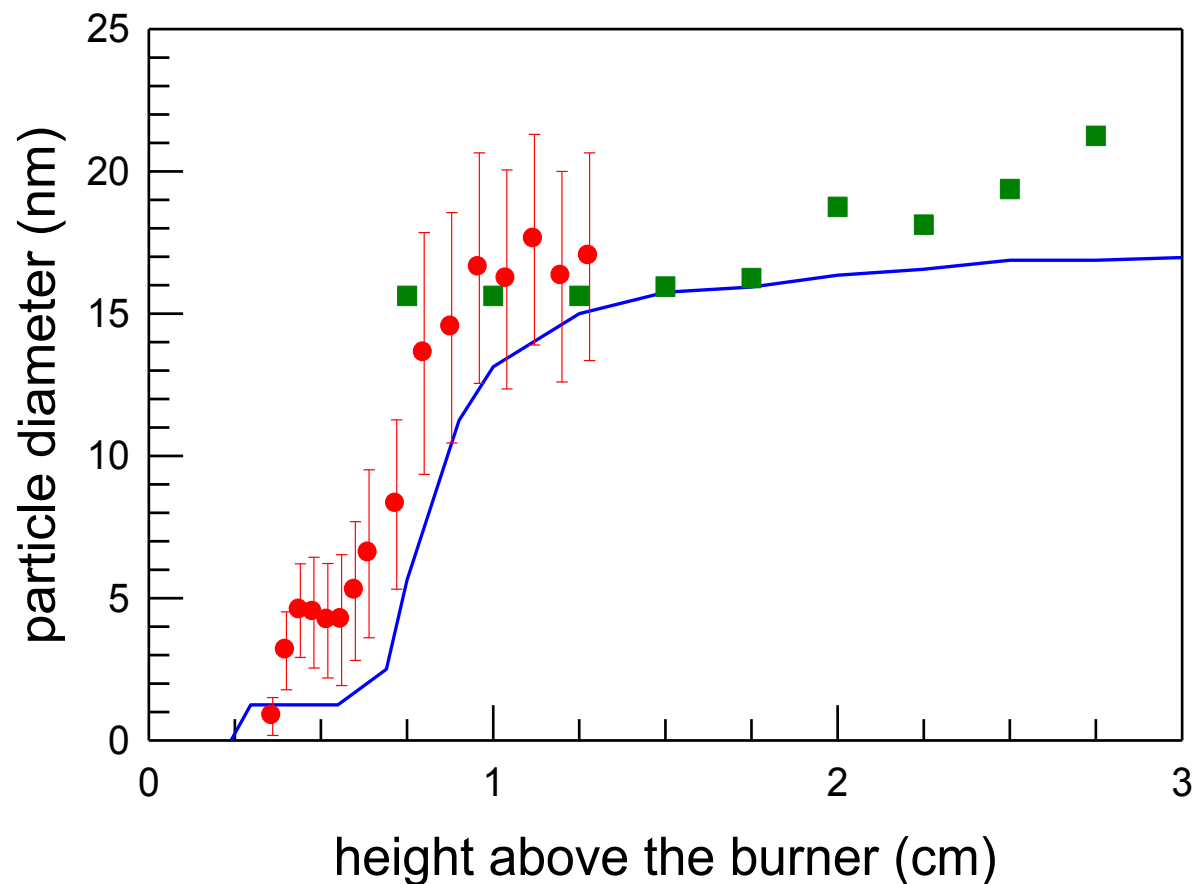
# Schultz Distribution: Analysis of Polydispersed SAXS Data

Example from soot studies



Polydispersity analysis of scattering data from self-assembled systems  
Eric Y. Sheu, *Phys. Rev. A* **45**, 2428-2438 (1992)

# Change in Soot Particle Size with Time (height) for a Toluene Flame

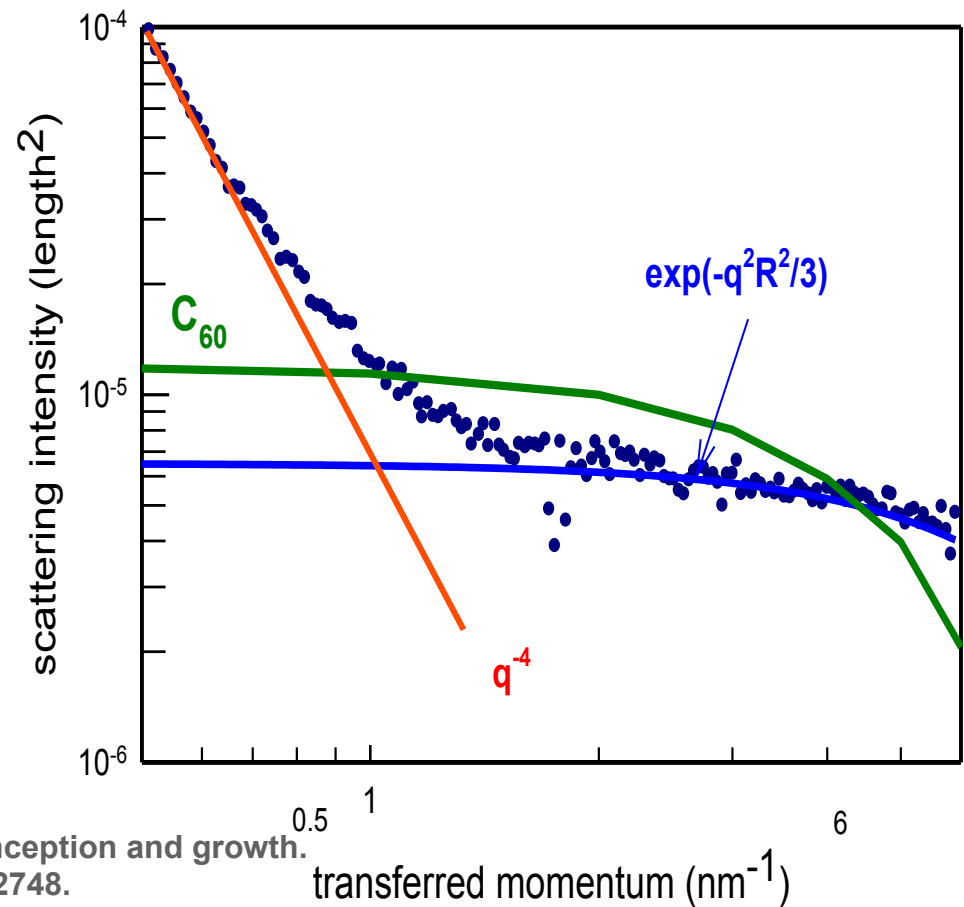


- Toluene Soot in a CO/Hydrogen Flame, Winans, Hessler, Seifert and Fletcher  
Height adjusted to match other data and model and the bars reflect the size distribution at each height
- 14% Ethylene in Air / Premixed, F. Xu, P. B. Sunderland, & G. M. Faeth  
*Combust. Flame* **108**, 472-493 (1997)
- Kinetic Model of Soot Formation, J. Appel, H. Bockhorn, & M. Frenklach  
*Combust. Flame* **121**, 122-136 (2000)

# Two Unique Distributions

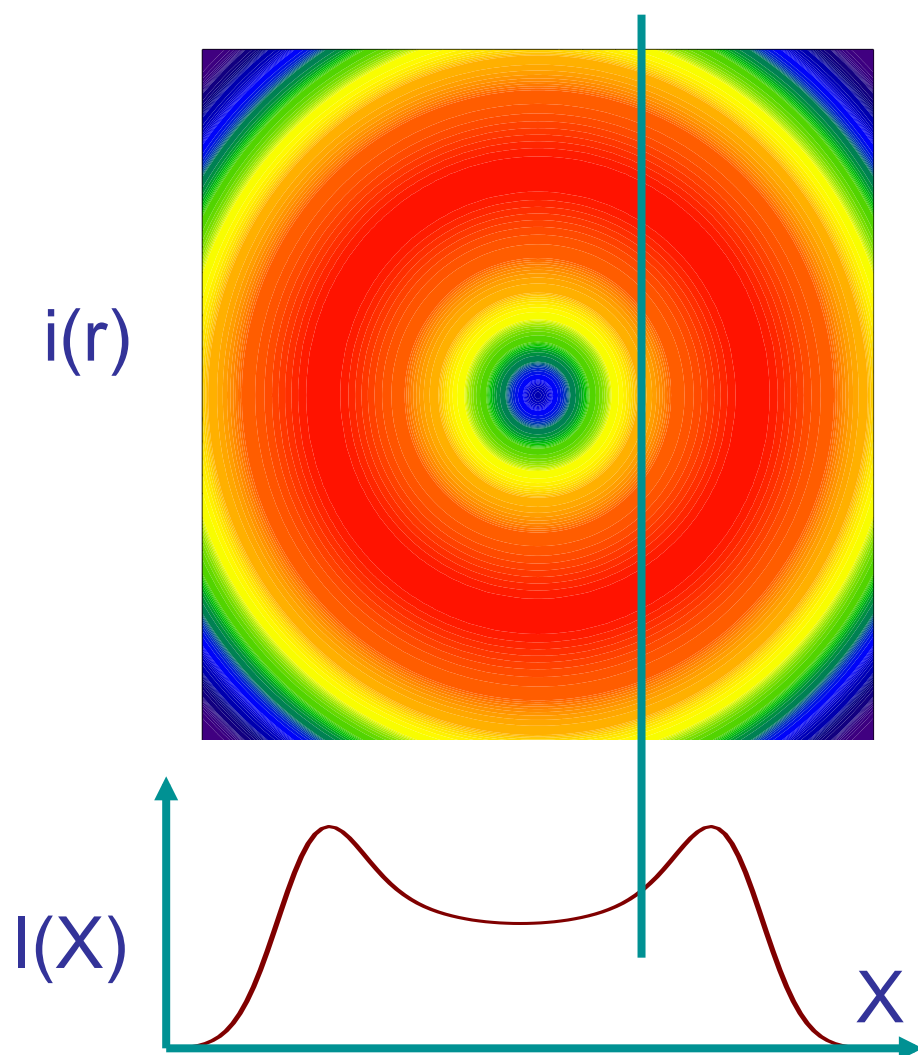
- All data can be modeled with only two species, primary particles (previously observed) and PAH species (new observation).
- **Smaller than  $C_{60}$ .**
- May be smallest structure observed by SAXS.
- Gas-phase systems have less background than liquids/solids.

## Sub-Nanoscale Soot Particles Propylene Diffusion Flame



Hessler, J. P.; Seifert, S.; Winans, R. E.  
Spatially resolved small-angle X-ray scattering studies of soot inception and growth.  
Proceedings of the Combustion Institute (2002), 29(Pt. 2), 2743-2748.

# Abel Inversion Calculate Radial Distribution



integrated scattering intensity

$$I(q, X) = 2 \int_X^{\infty} \frac{ri(q, r)}{\sqrt{r^2 - X^2}} dr$$

local scattering intensity

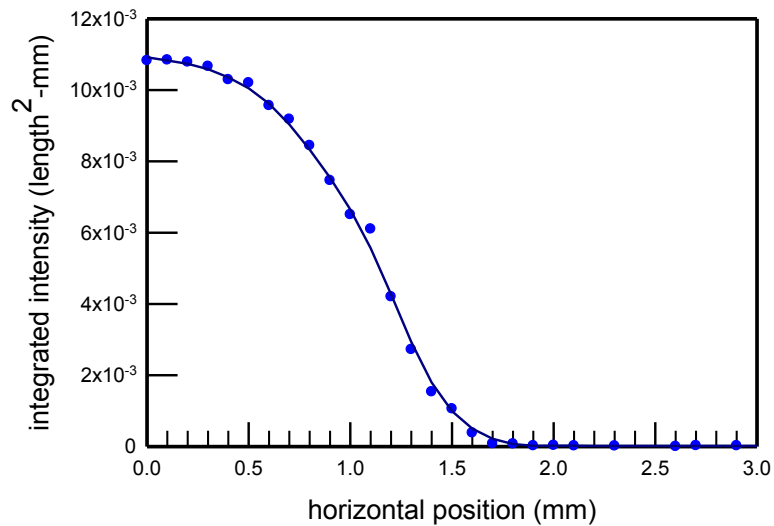
$$i(q, r) = -\frac{1}{\pi} \int_r^{\infty} \left[ \frac{dI(q, X)}{dX} \right] \frac{dX}{\sqrt{X^2 - r^2}}$$

H. R. Griem, 1964, McGraw-Hill  
*Plasma Spectroscopy*, pp. 176-178  
C. J. Dasch  
*Appl. Opt.* **21**, 1146 (1992).

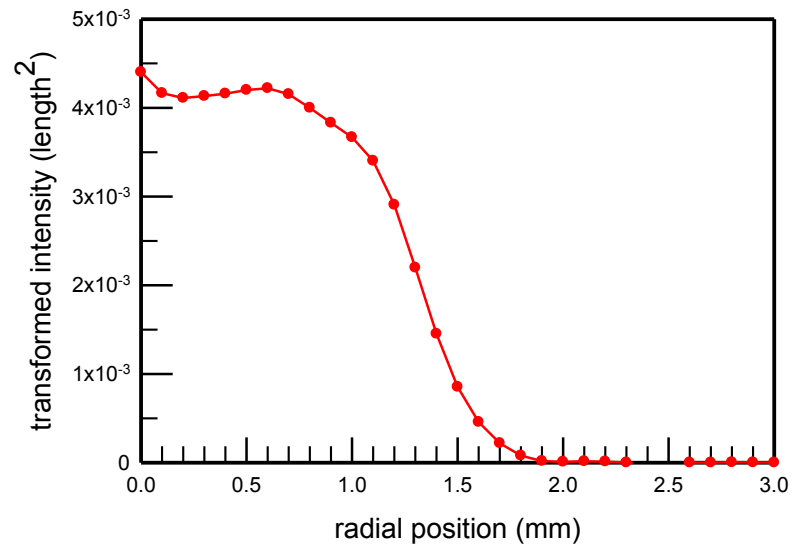


# Abel Inversion: Example

Observed line-of-sight  
integrated intensity,  $I(q,x,z)$

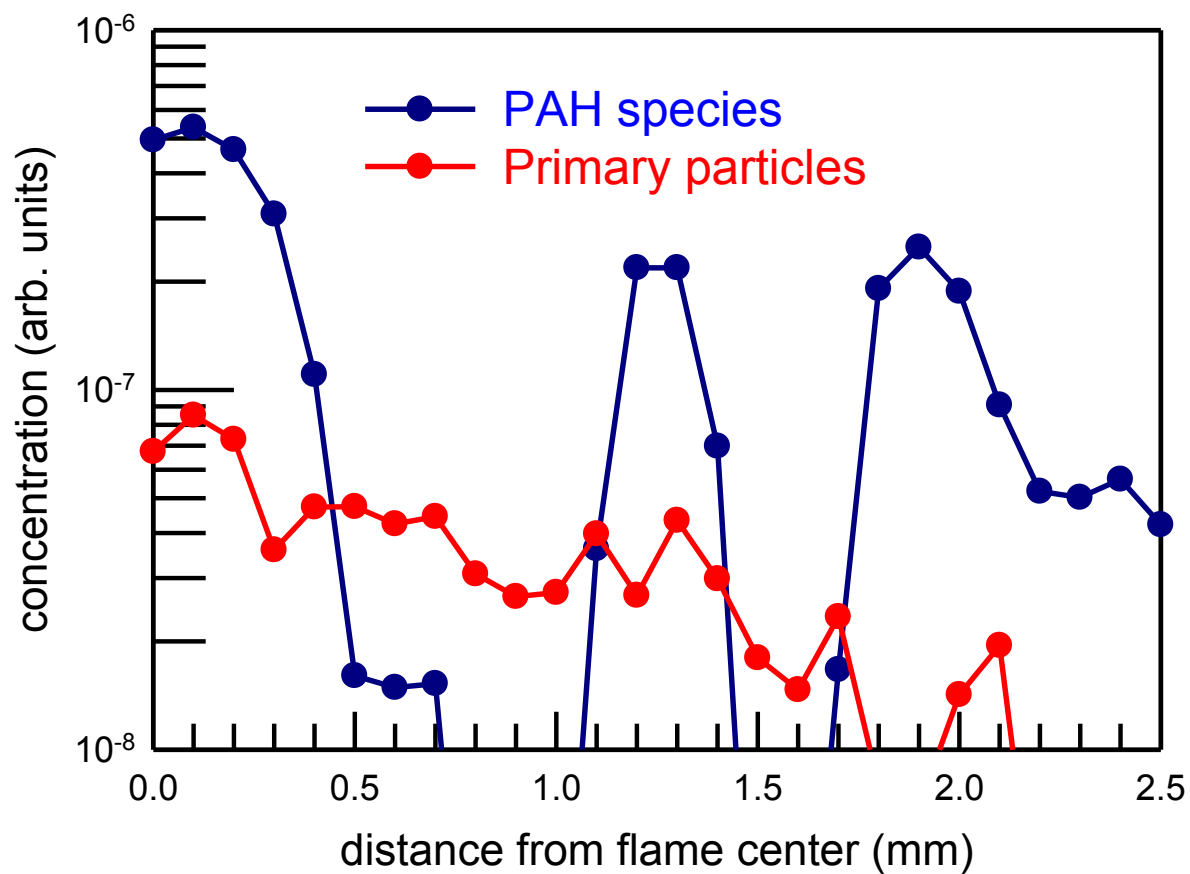


Calculated local  
scattering intensity,  $i(q,r,z)$



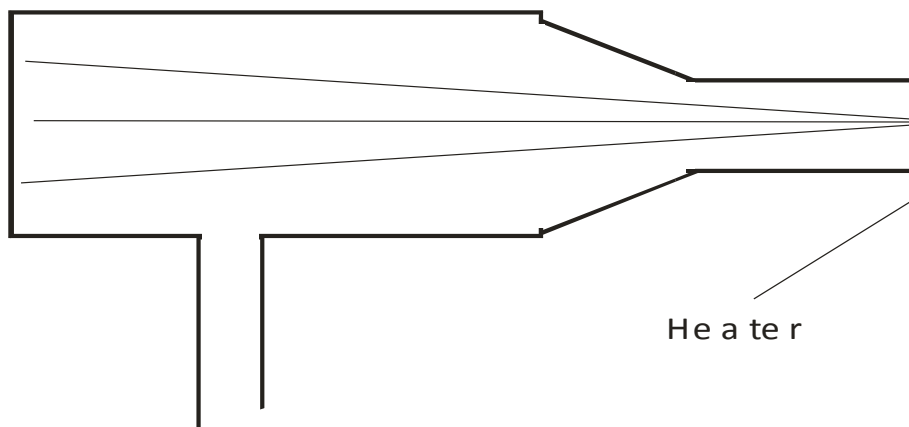
- Reflect about origin and average
- Perform four-point numerical smoothing with  $I = 0$  at the boundary.
- Cameron J. Dasch, *Appl. Opt.* 1992, **31**, 1146-1152

## *Rainbow Structure - Propylene Diffusion Flame*



# *PAH Sampling for Small Angle Scattering With a Static Cell*

De t e c t o r



Va c u u m

M i c a w i n d o w s

*X-rays*

Q u a r t z C e l l

H e a t e r

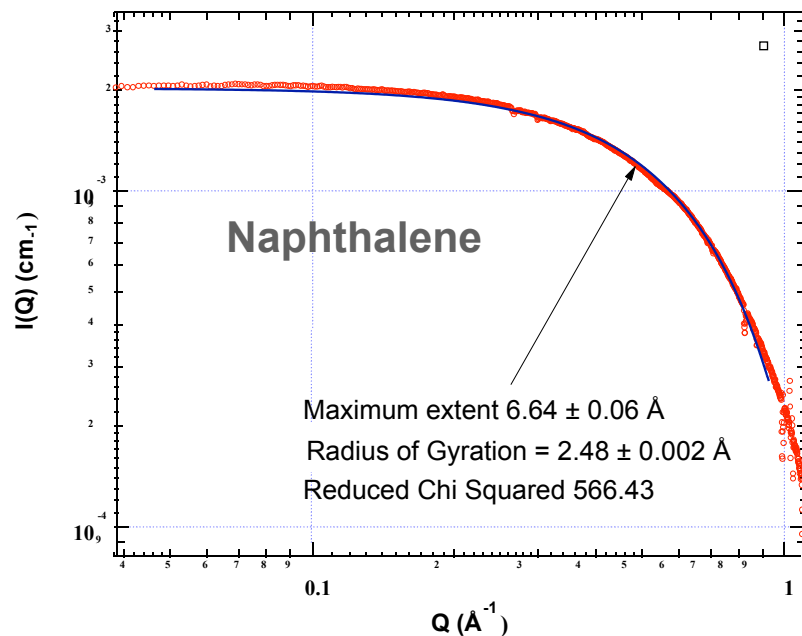
H e l i u m f l o w



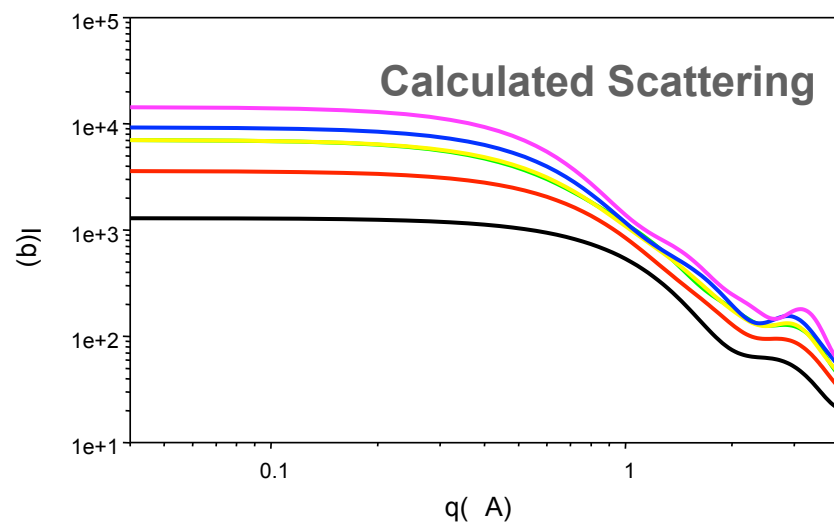
# Analysis of Static Cell PAH Scattering

Moore, P. B. *Journal of Applied Crystallography* **1980**, 13, 168-75

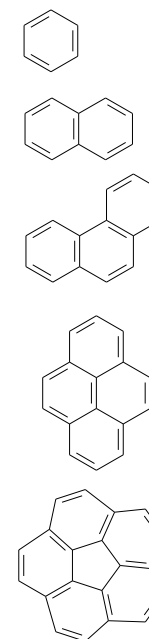
Fit using Moore's indirect Fourier transform









Molecule	Rg (Å)		Maximum Extent (Å)	
	Measured	Calculated	Measured	Calculated
Benzene	1.64	1.52	3.71	4.30
Naphthalene	2.48	2.02	6.64	6.50
Phenanthrene	3.11	2.55	7.92	8.60

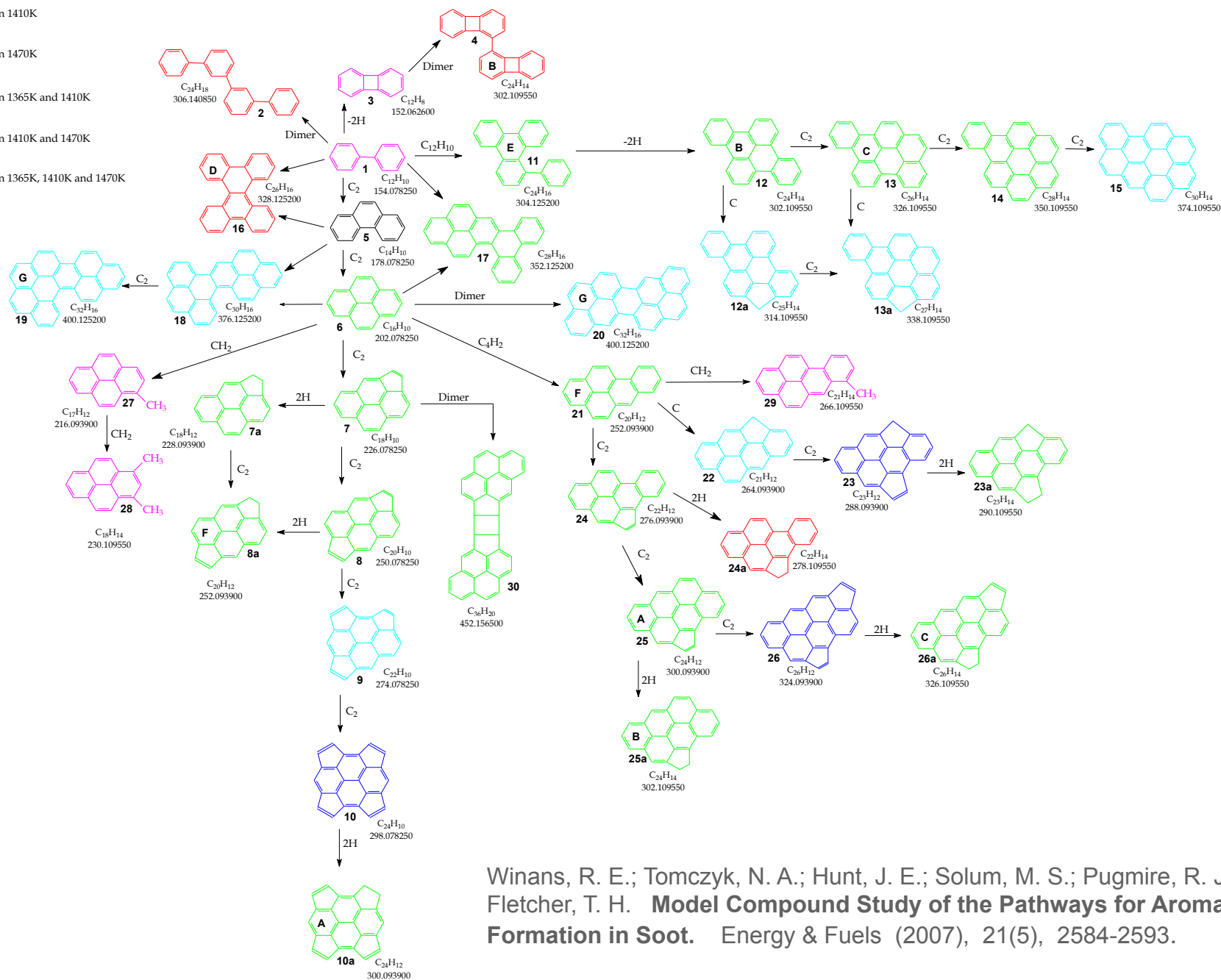


— Benzene(1.52)  
 — Naphthalene (2.11)  
 — Phenanthrene (2.55)  
 — Pyrene (2.56)  
 — Corannulene (2.725)



-  Found in 1365K
-  Found in 1410K
-  Found in 1470K
-  Found in 1365K and 1410K
-  Found in 1410K and 1470K
-  Found in 1365K, 1410K and 1470K

## Scheme I



Winans, R. E.; Tomczyk, N. A.; Hunt, J. E.; Solum, M. S.; Pugmire, R. J.; Jiang, Y. J.; Fletcher, T. H. **Model Compound Study of the Pathways for Aromatic Hydrocarbon Formation in Soot.** *Energy & Fuels* (2007), 21(5), 2584-2593.

# Conclusions

- **Small soot precursor molecules** from toluene can be observed by SAXS.
- Soot growth can be measured by SAXS.
- Highly dispersed molecular sizes.
- Initially observed layered molecules that become more disordered and 3D with time.
- There are two distinct size regions with small PAH observable by SAXS.



# ***CO<sub>2</sub> and Coal Issues***

- It is thought that CO<sub>2</sub> dissolves in coal
- Coal swells in CO<sub>2</sub>
- Pore structure of coals is variable (molecular to visible holes) and rank dependent – need to be able to access broad range of pore sizes ( Angstroms -> microns )

Romanov, Vyacheslav N.; Goodman, Angela L.; Larsen, John W.. Errors in CO<sub>2</sub> Adsorption Measurements Caused by Coal Swelling. *Energy & Fuels* (2006), 20(1), 415-416.

Goodman, A. L.; Favors, R. N.; Hill, M. M.; Larsen, John W.. Structure Changes in Pittsburgh No. 8 Coal Caused by Sorption of CO<sub>2</sub> Gas. *Energy & Fuels* (2005), 19(4), 1759-1760.

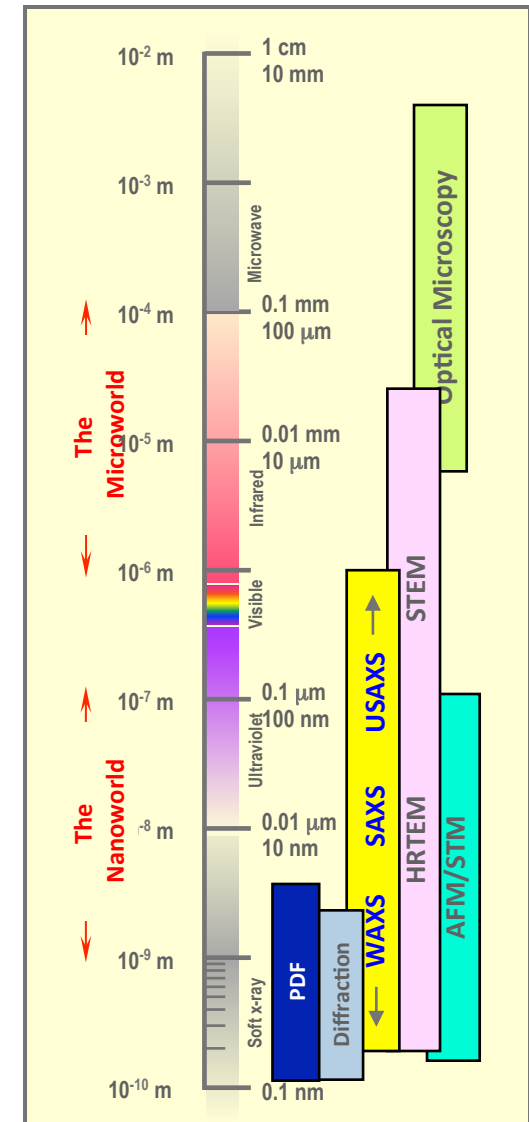
Larsen, John W.. The effects of dissolved CO<sub>2</sub> on coal structure and properties. *International Journal of Coal Geology* (2004), 57(1), 63-70.



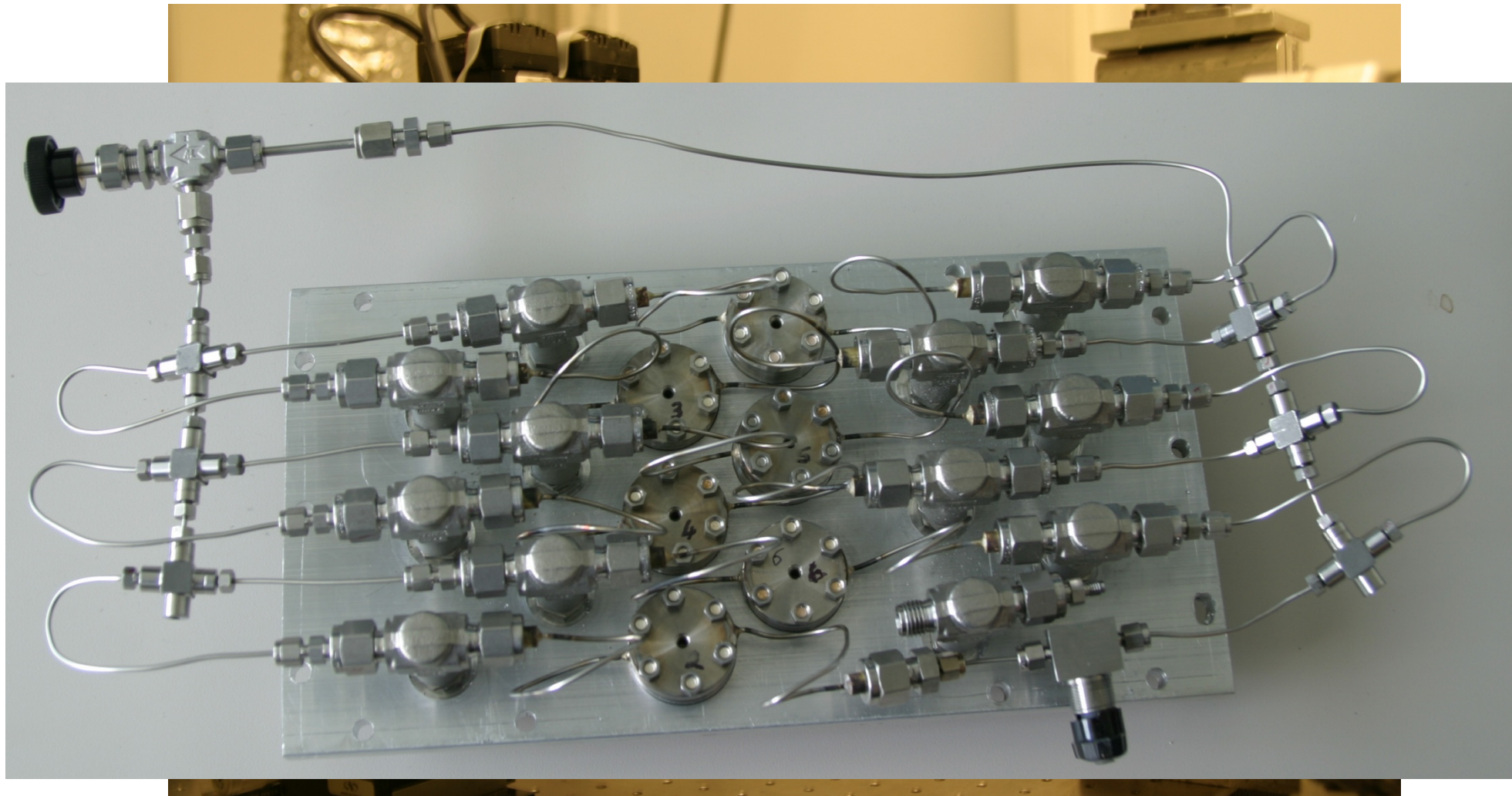
# Small Angle X-ray Scattering Analysis of Coal Structure

- SAXS provides pore size, size distribution, shape and surface morphology over broad length scales.
- SAXS is an in situ technique and can work with a variety of high pressure cells.
- SAXS has been used to follow changes in coal structure in gasification and solvent swelling.

Calo, J. M.; Hall, P. J.; Houtmann, S.; Lozano-Castello, D.; Winans, R. E.; Seifert, S. "Real time" determination of porosity development in carbons: A combined SAXS/TGA approach. *Studies in Surface Science and Catalysis* (2002), 144(Characterization of Porous Solids VI), 59-66.

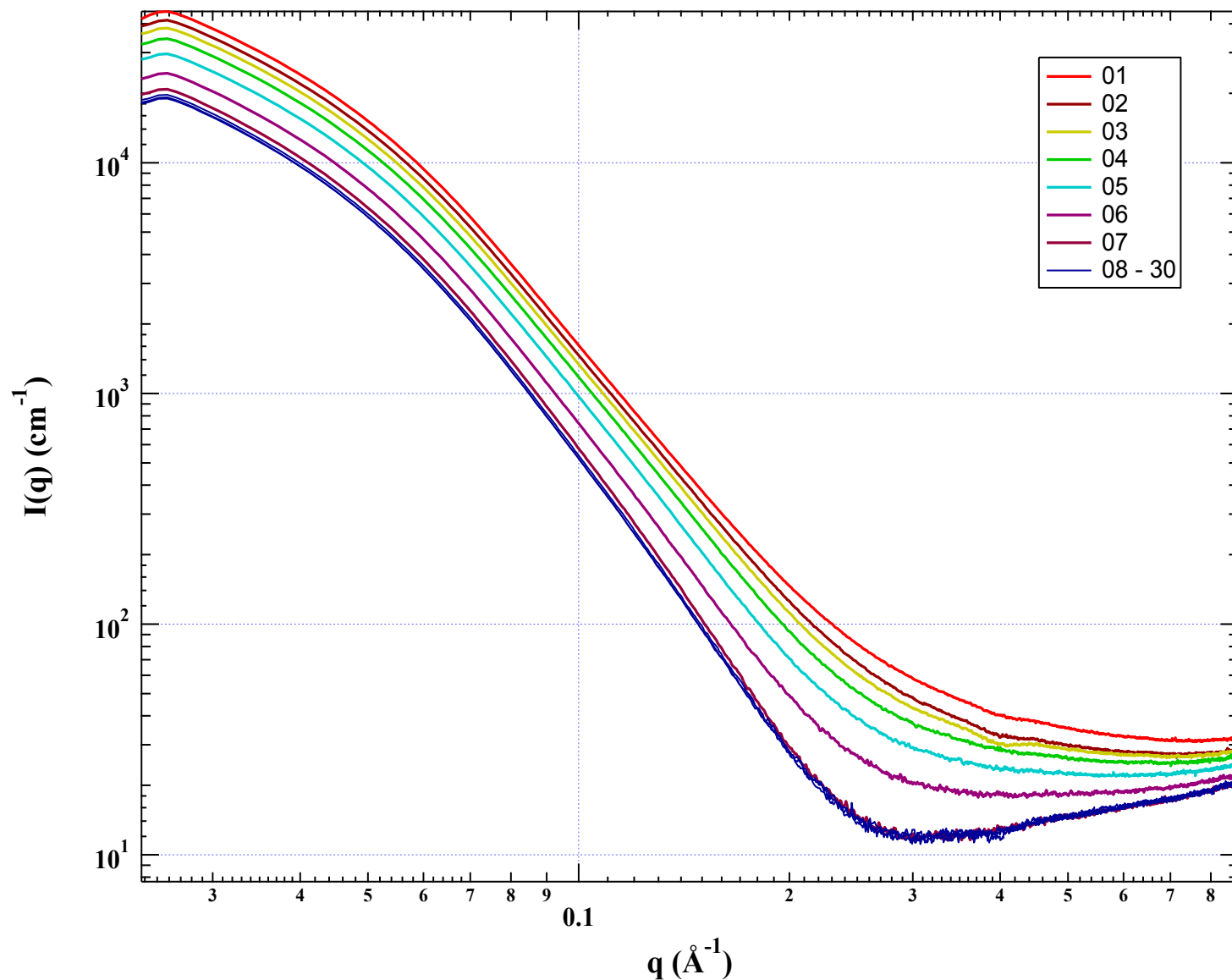


# SAXS Instruments at 12ID

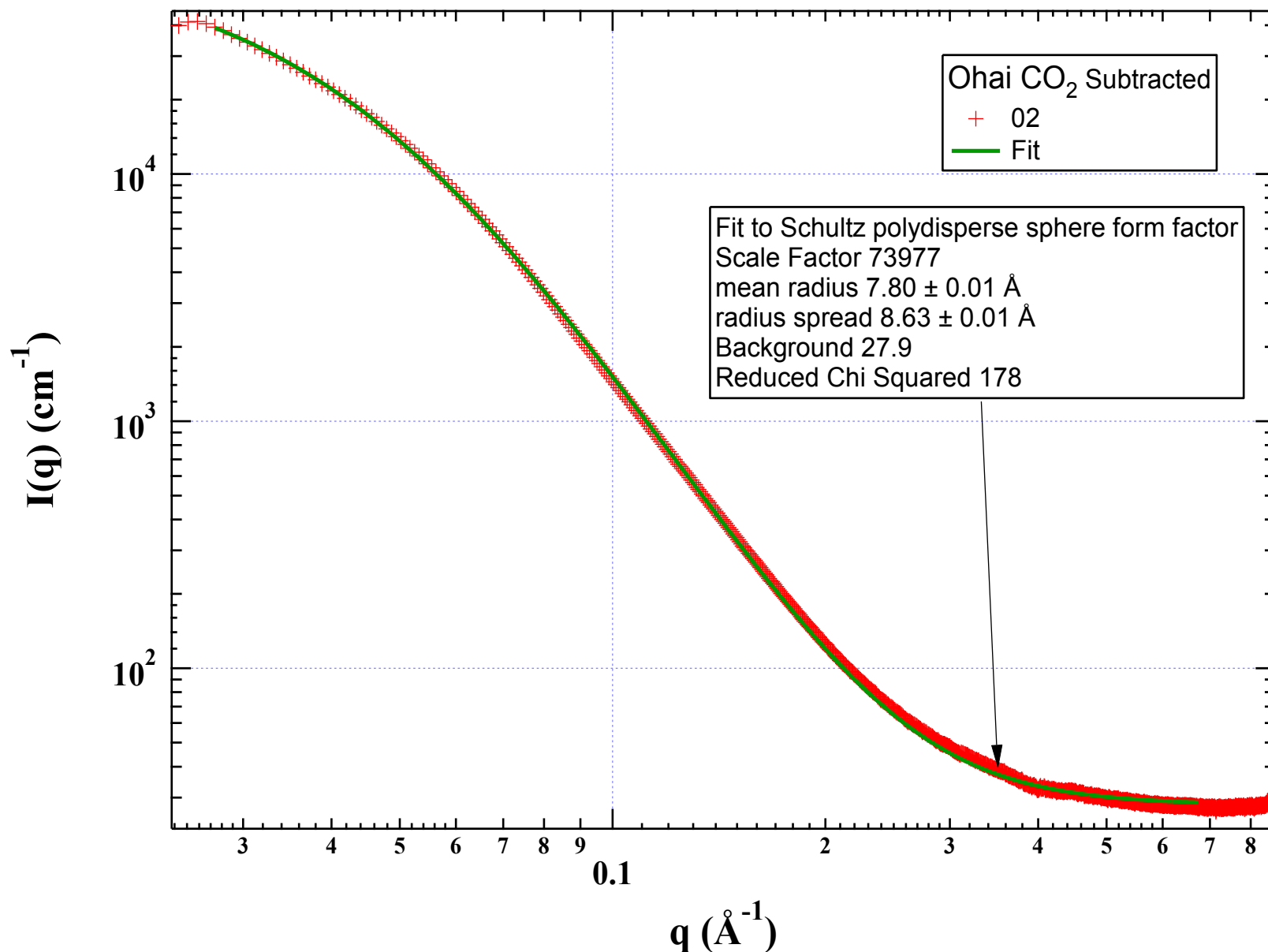


# Ohai Subbituminous Coal

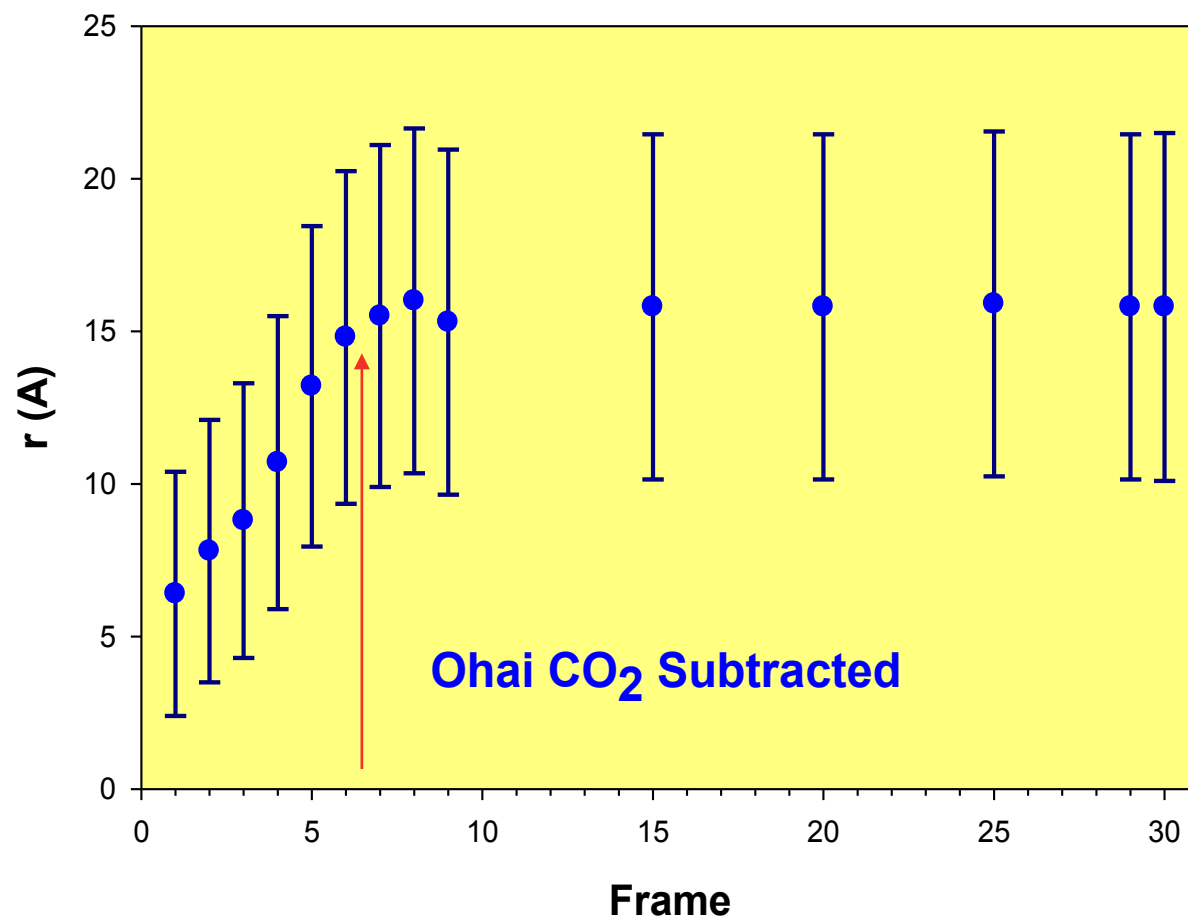
CO<sub>2</sub> increased from 150 to 800 psi, CO<sub>2</sub> blank subtracted



# Ohai Coal - Schulz Polydispersed Spheres

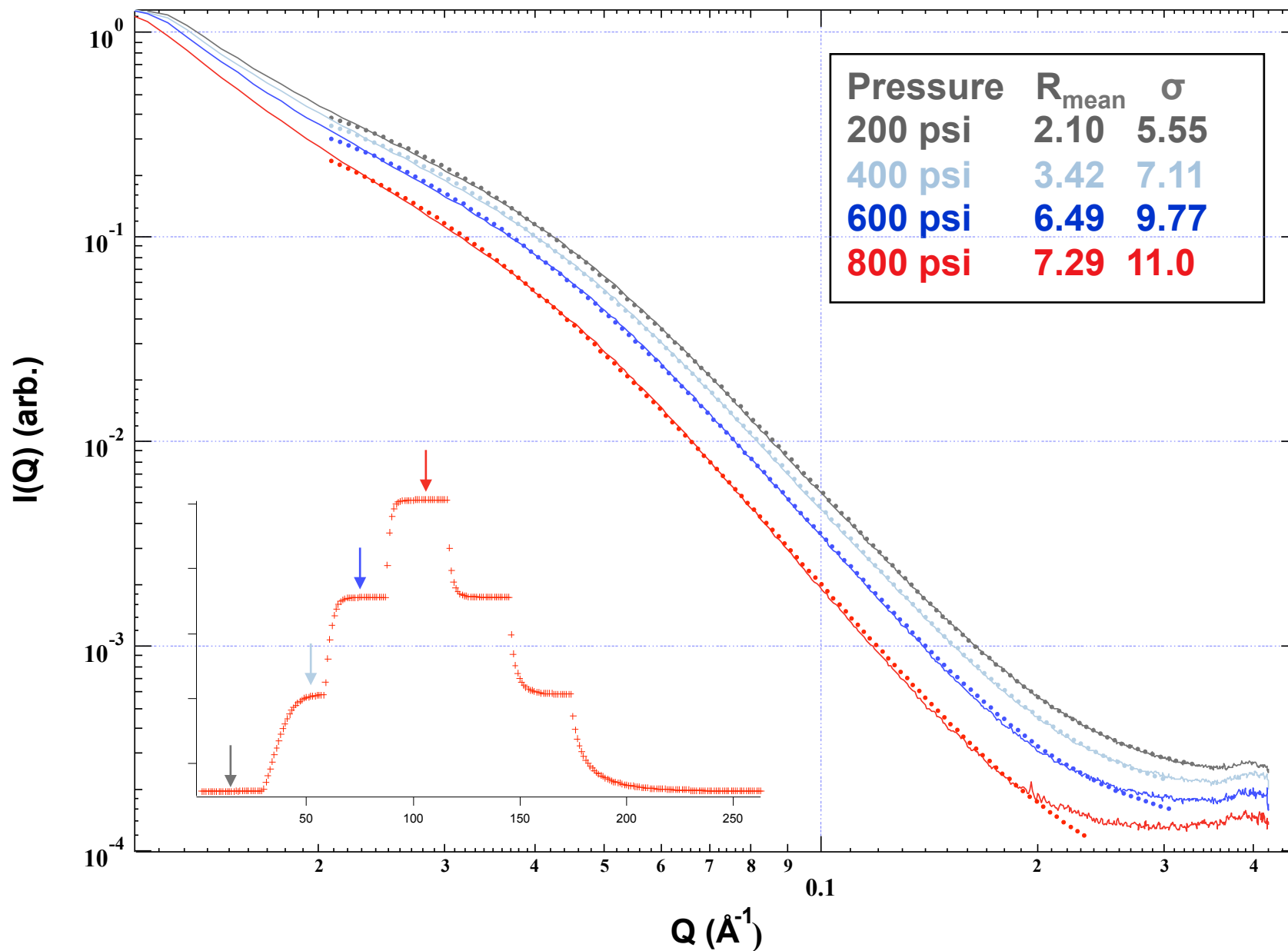


# Ohai Coal - Schulz Polydispersed Spheres



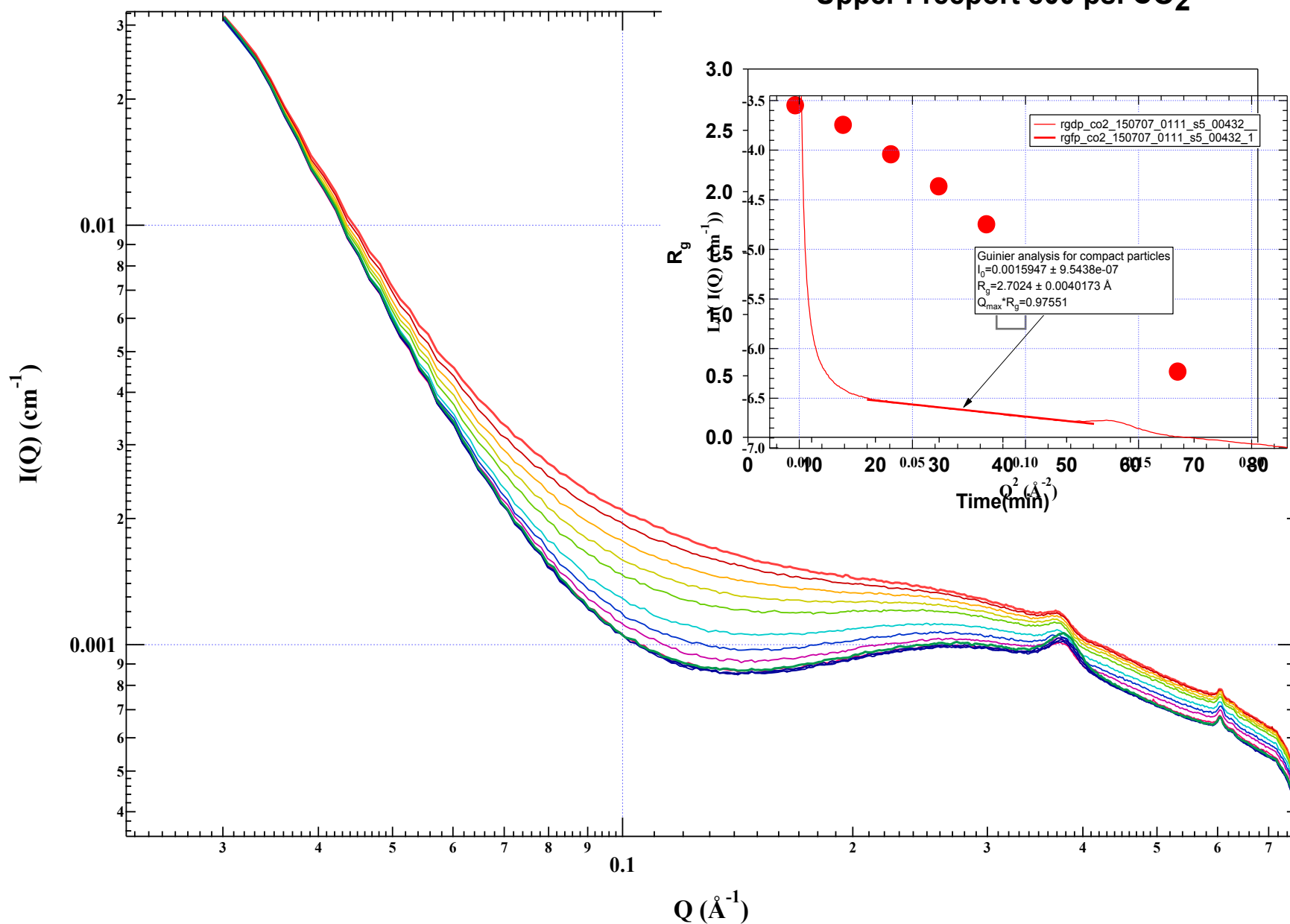
# Illinois No. 6 Bituminous Coal – APCS 3

Fit to Schultz polydisperse sphere form factor



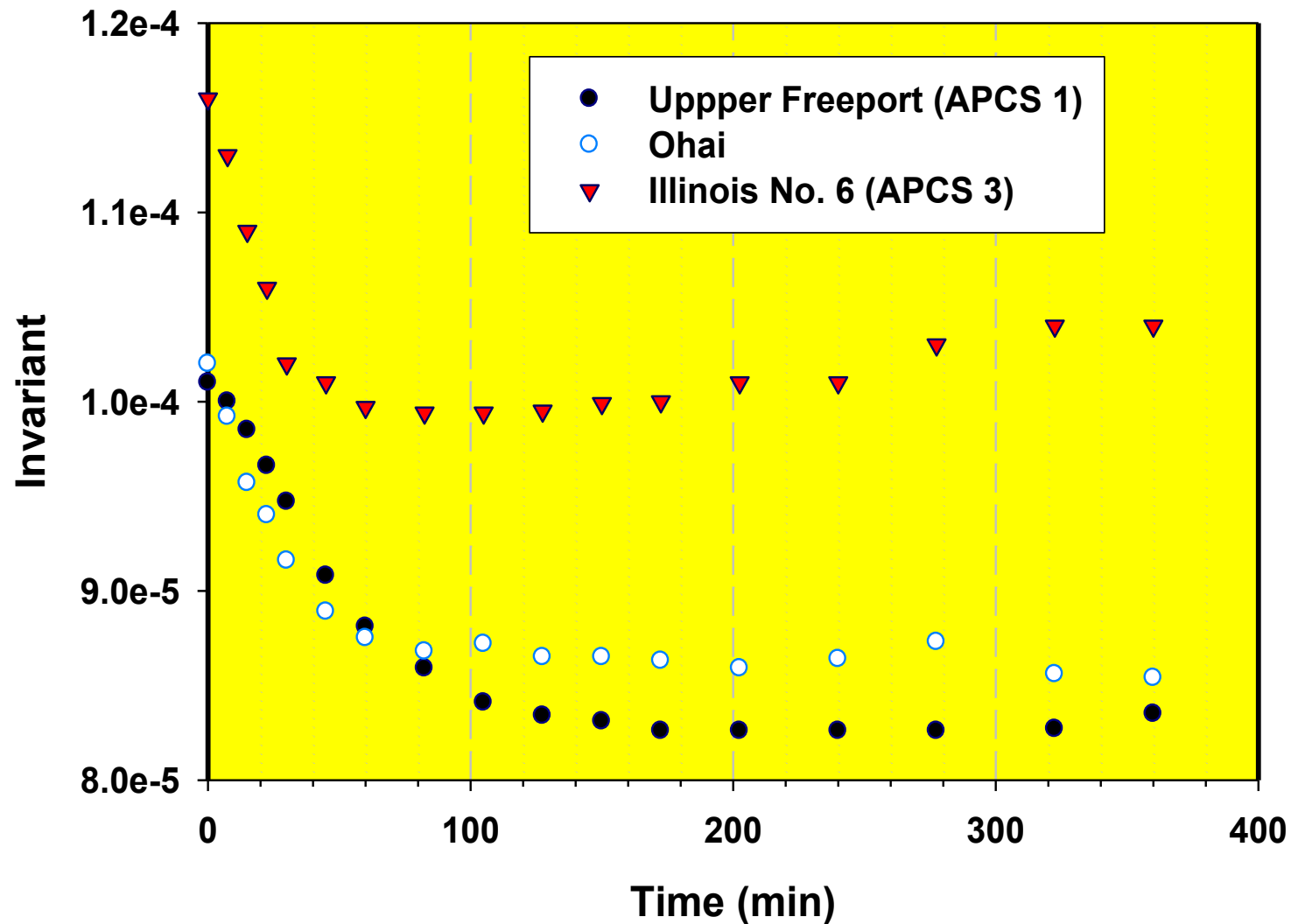
# Upper Freeport APCS 1 – 800 psi

## Upper Freeport 800 psi CO<sub>2</sub>





## Invariant Calculated for Coals at 900 psi



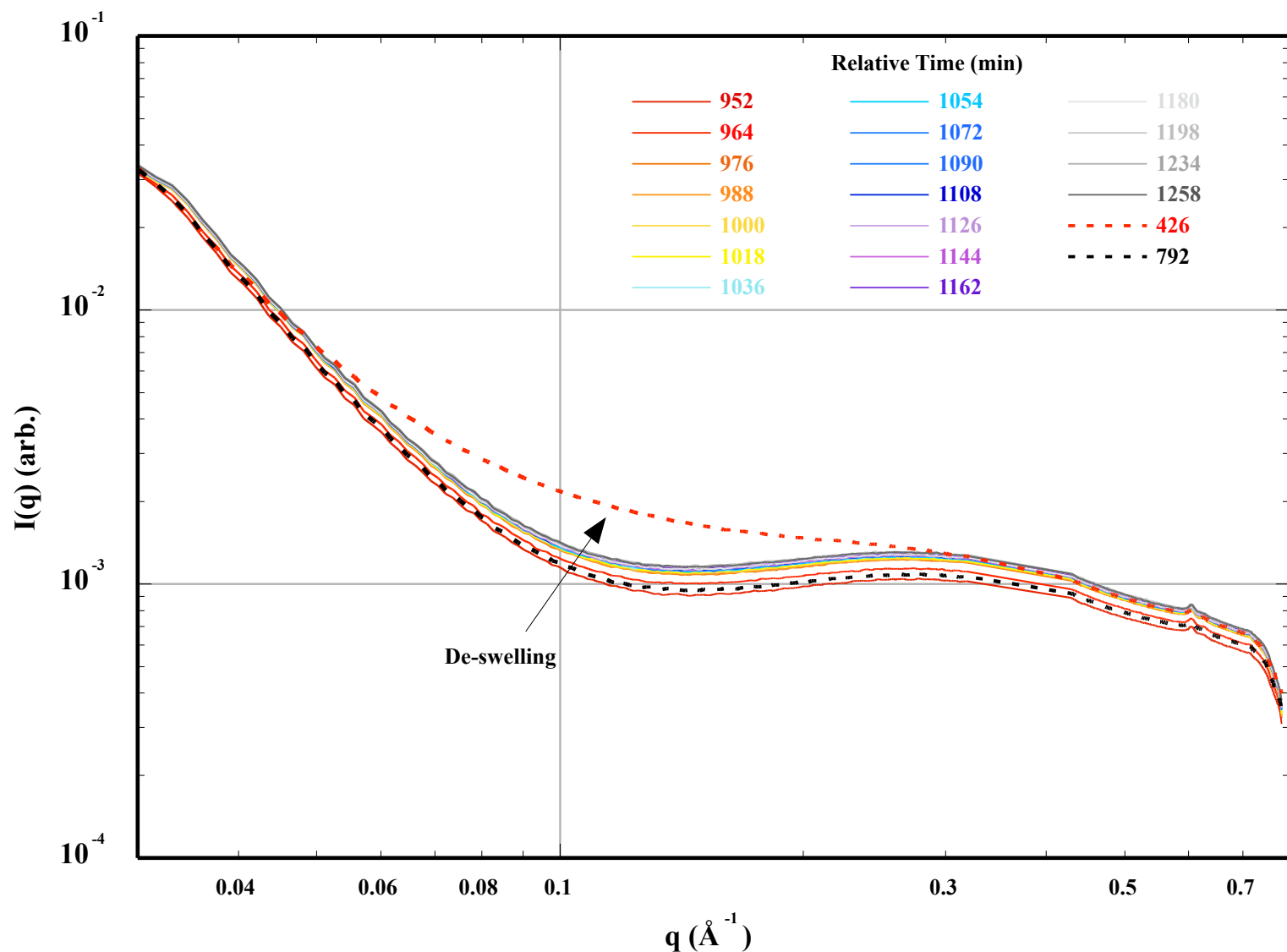
$$Q = \int_0^{\infty} q^2 dq \cdot I(q)$$

Decrease in the invariant is the result of a decrease in difference in electron density, which occurs as the CO<sub>2</sub> is filling the pores.

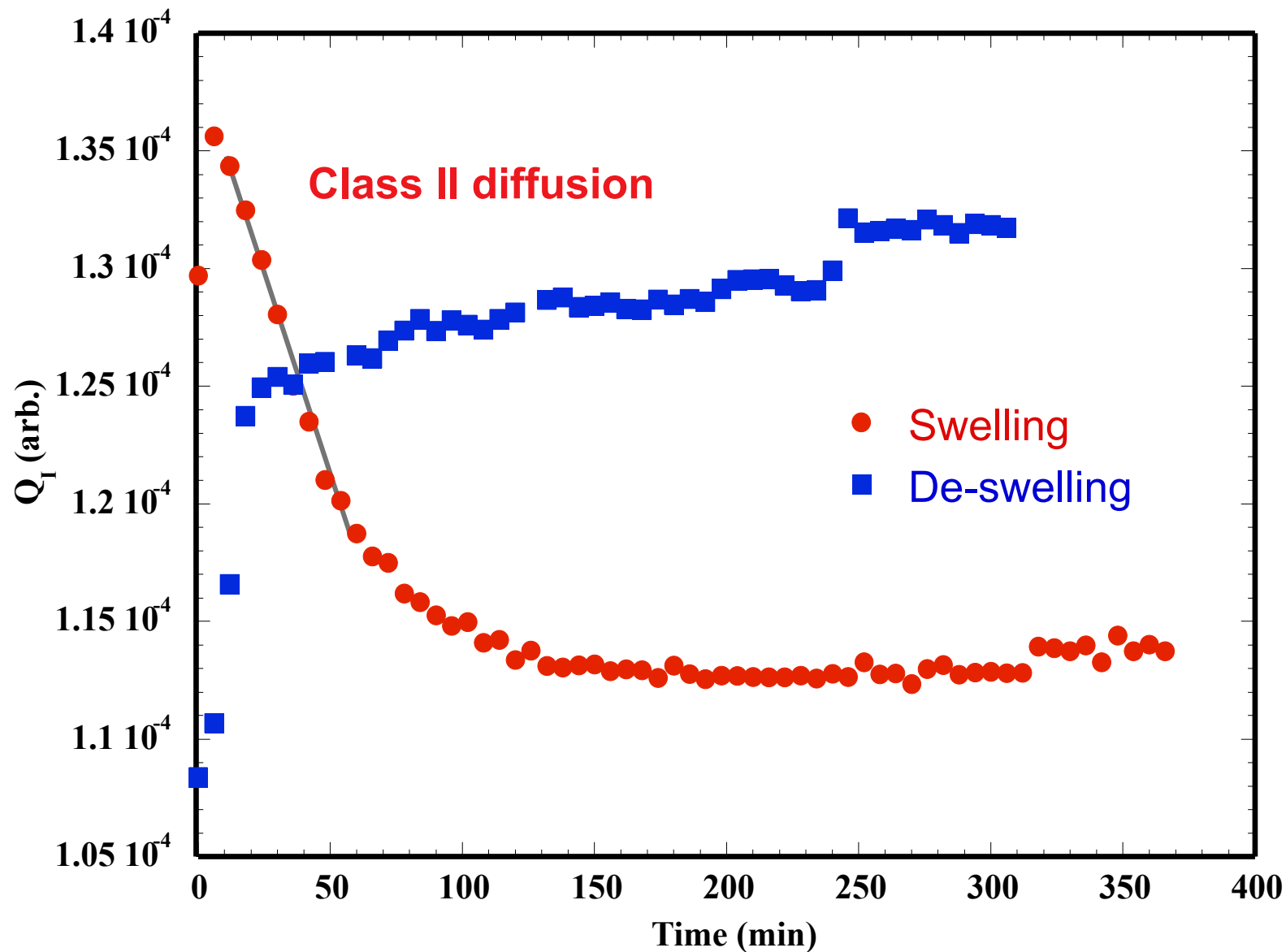


## Upper Freeport APCS 1 – 800 psi

Scattering intensity of the APCS 1 coal following depressurization of the sample cell to atmospheric pressure air from 800 psig CO<sub>2</sub> at ambient temperature.



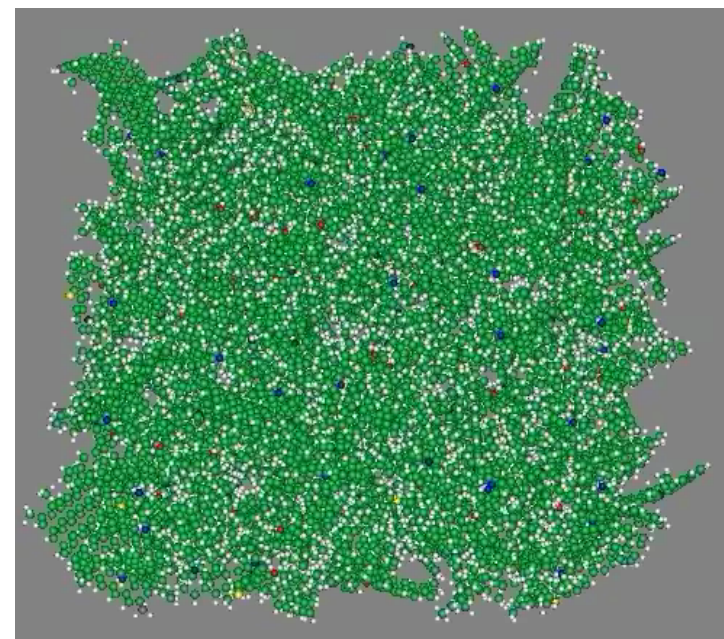
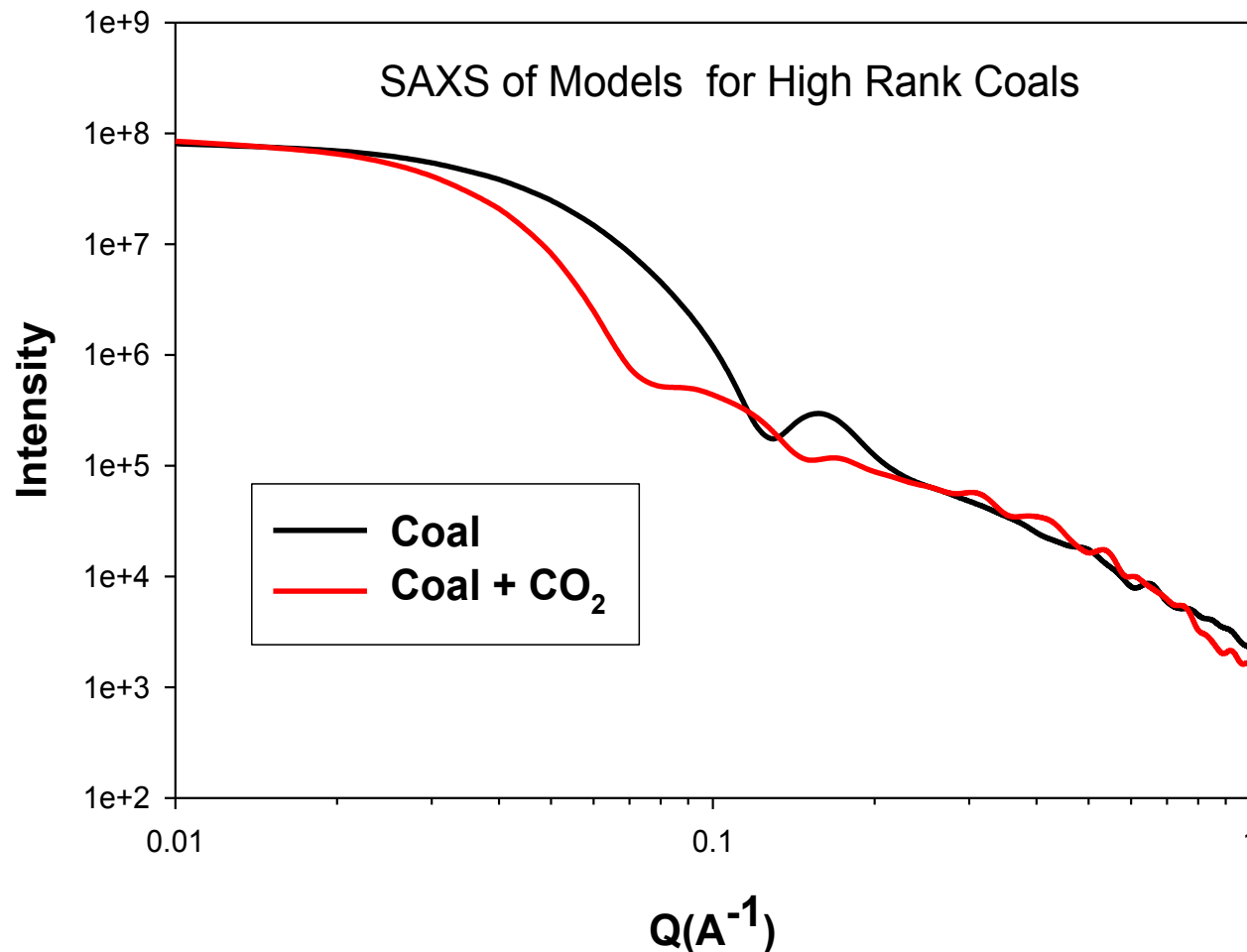
## Upper Freeport APCS 1 – 800 psi - Invariant



# SAXS Calculated from Coal Models

SAXS calculated using CRY SOL

Svergun D.I., Barberato C. & Koch M.H.J. (1995)  
J. Appl. Cryst., 28, 768-773.



Models from:

Narkiewicz, M. R. and Mathews, J. P. Visualization of carbon dioxide sequestration issues within coal using a molecular representation of Pocahontas No. 3 coal, 12th International Conference on Coal Science and Technology, 2005, October 9-14, Okinawa, Japan

# Conclusions

- In higher rank coals observed a slow uptake of CO<sub>2</sub> with a decrease in porosity.
- Model for CO<sub>2</sub> uptake in a high rank coal qualitative agrees with SAXS results
- Rank dependence is again observed in long exposures to CO<sub>2</sub>

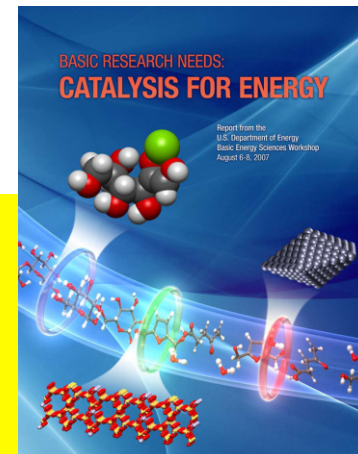


## Measurements in reaction environments

Measurements under catalytic reaction conditions are challenging because:

- a. Temperatures and pressures are often high
- b. Catalyst structures are complex
- c. Multiple phases containing the catalysts, reactants, and
- d. products are usually present

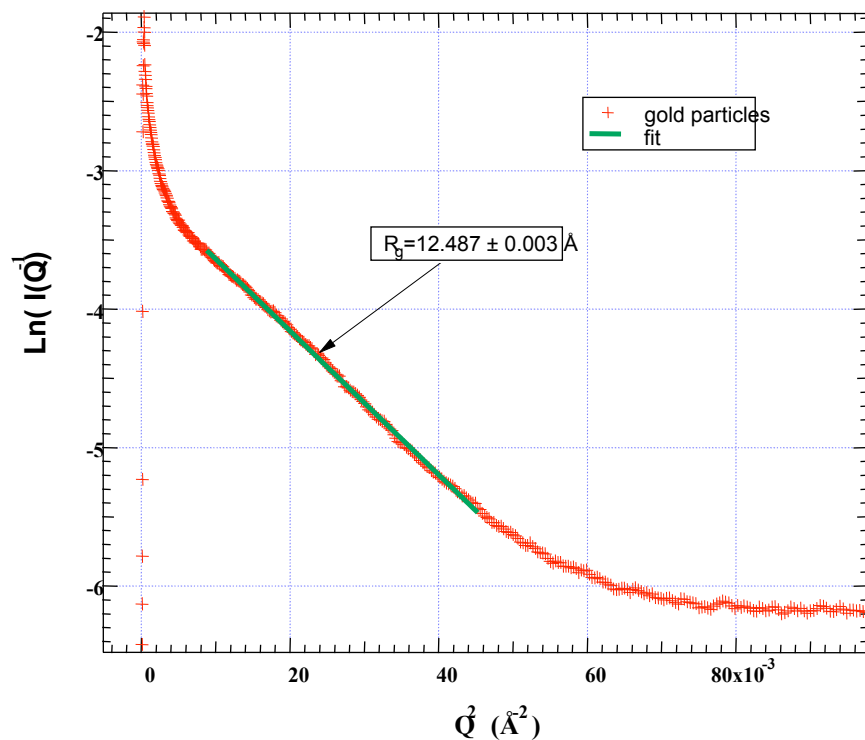
**Key structural information characterizing the catalyst and its surface species must be extracted from the maze of information in such complex mixtures.**



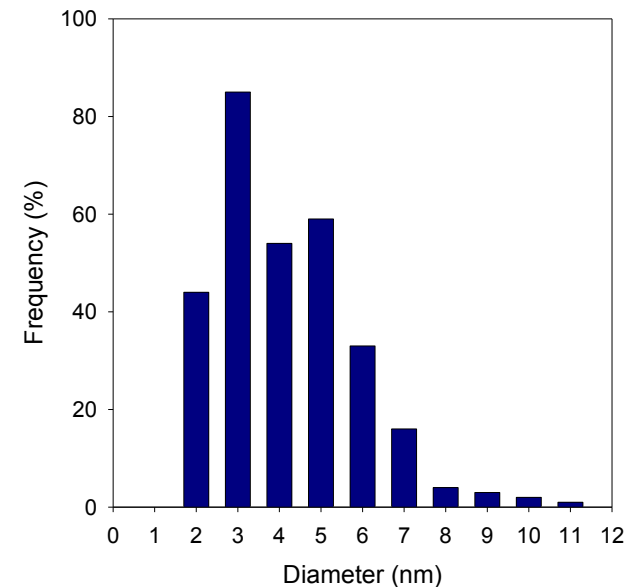
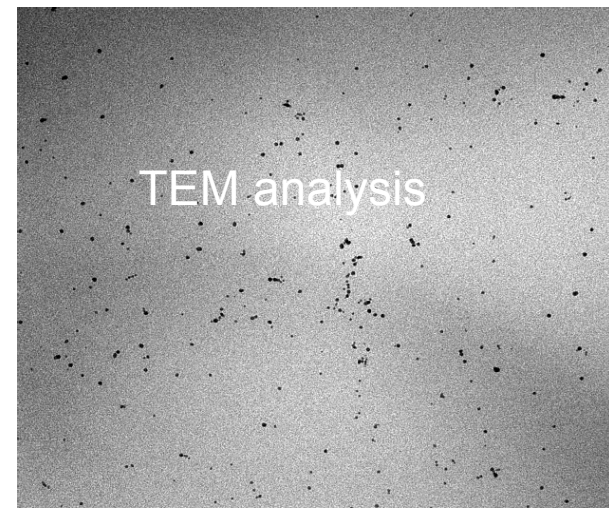
# Catalysis Studies

## Comparison of SAXS and TEM for Analysis of Micellar Gold Particles

Guinier analysis of SAXS data for a solution of gold particles in AOT micellar solution



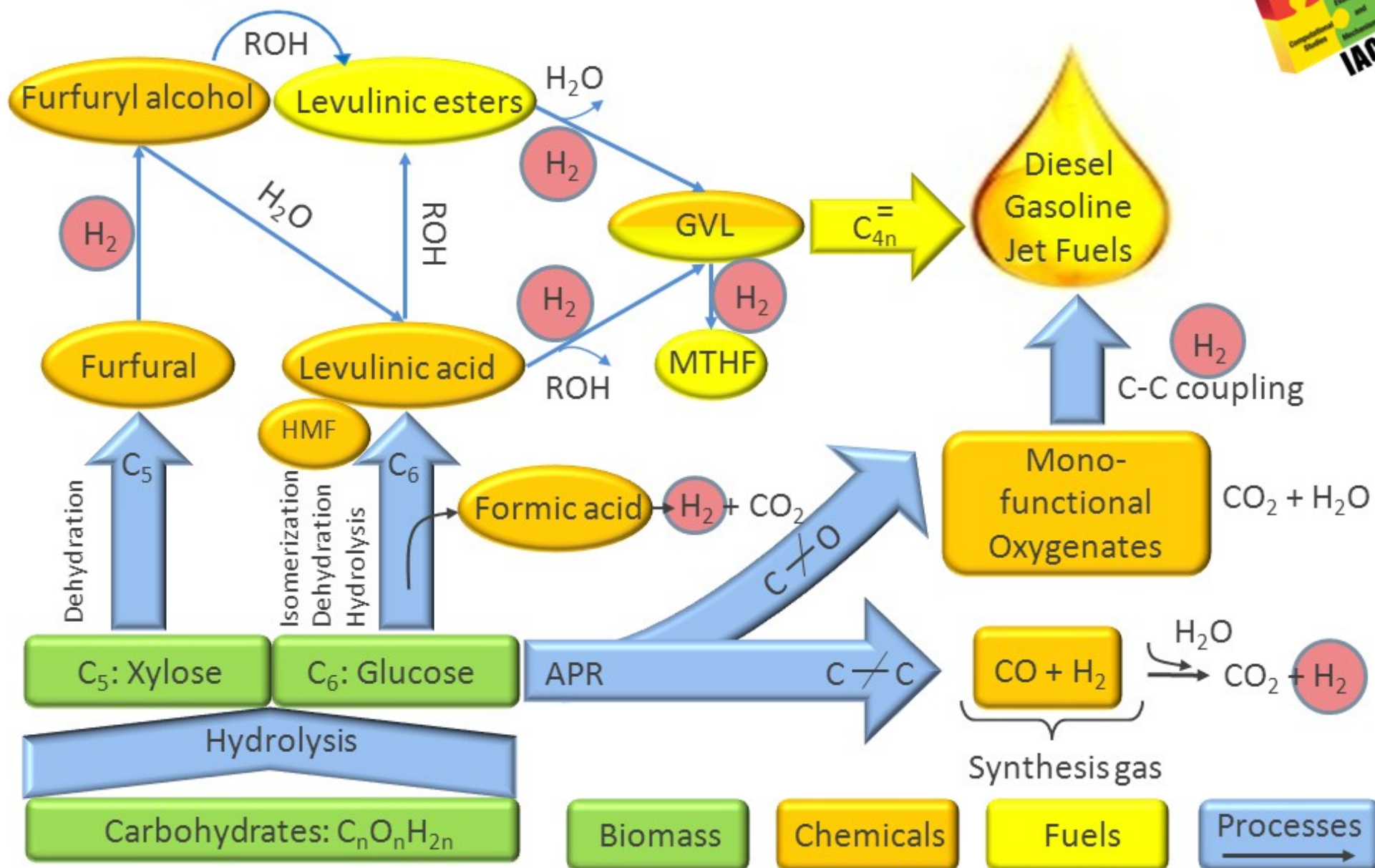
$$D = 2R_g * 1.29 = 3.2 \text{ nm}$$



$$D_{\text{ave}} = 4.17 \pm 1.7 \text{ nm}$$



# Roadmap to Fuels and Chemicals

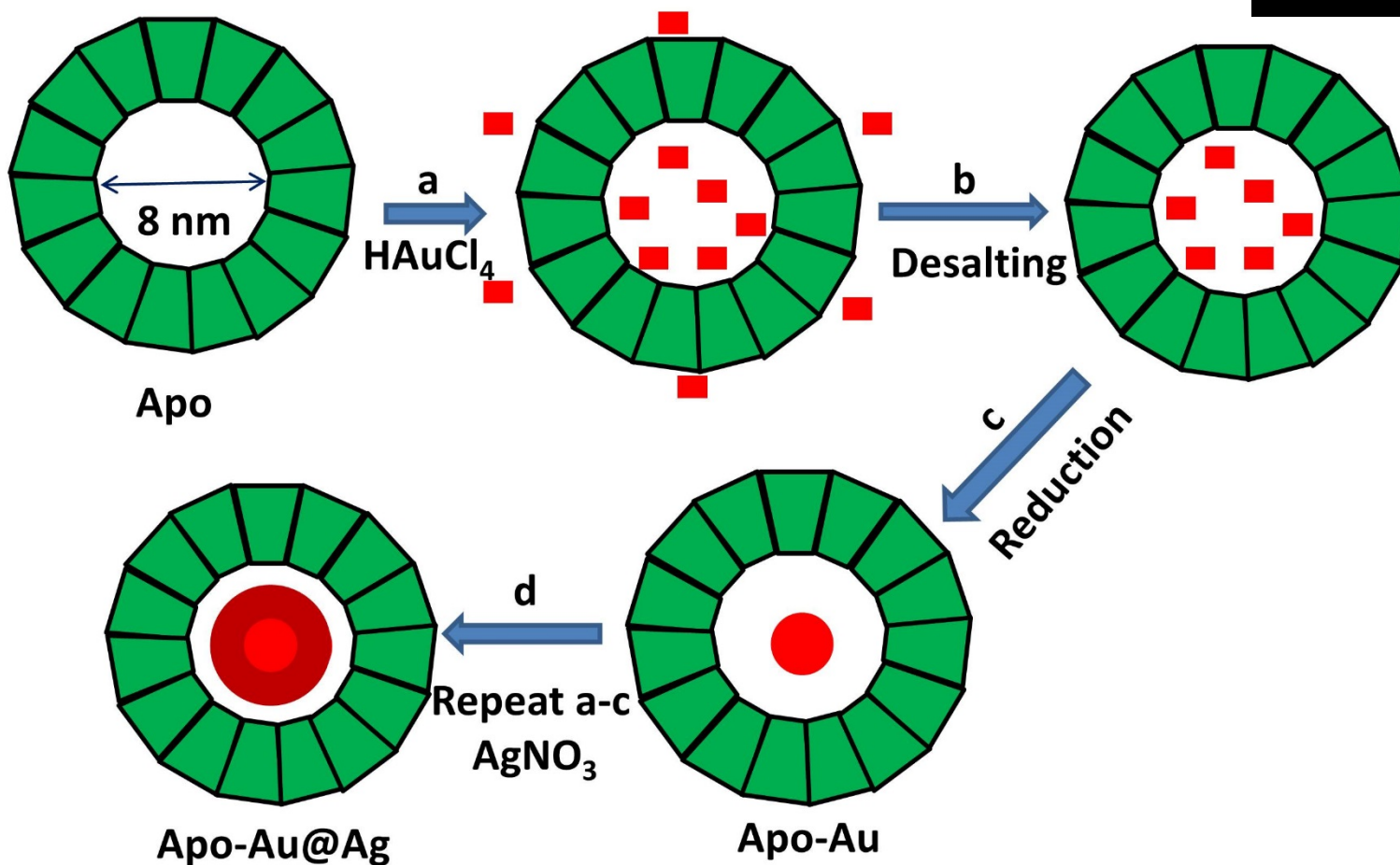
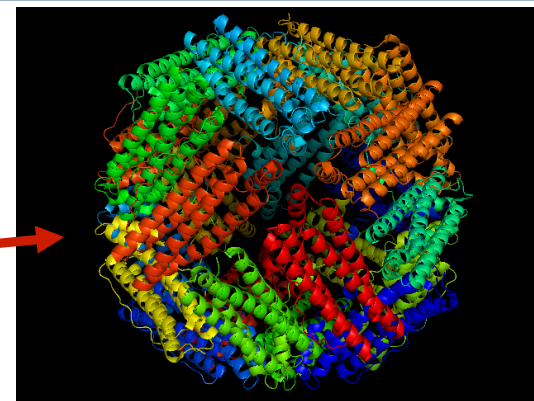


Institute for Atom-efficient Chemical Transformations (IACT)

Supported by US Department of Energy, Office of Basic Energy Sciences as part of an Energy Frontier Research Center

## *A Novel Nanobio Catalyst for Biofuels*

Synthesis of Au-core Ag-shell  
nanocatalyst within Apo ferritin



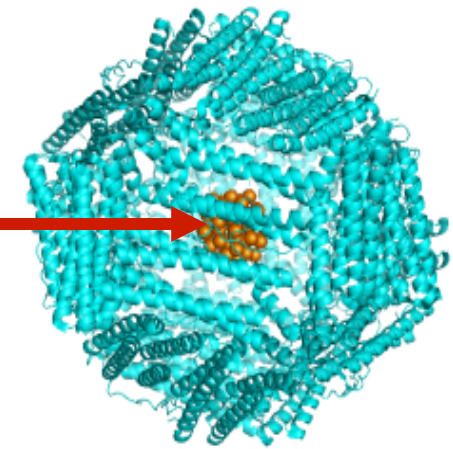
Li, T.; Chattopadhyay, S.; Shibata, T.; Cook, R. E.; Miller, J. T.; Suthiwangcharoen, Ni.; Lee, S.; Winans, R. E.; Lee, B. *Journal of Materials Chemistry* (2012), 22(29), 14458-14464.



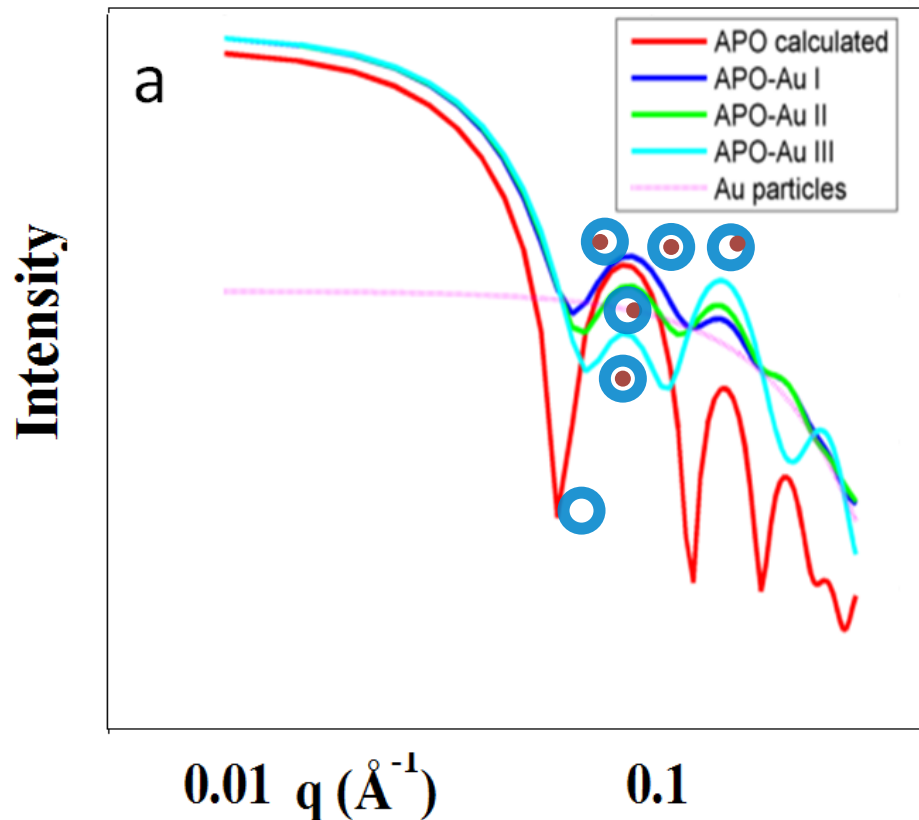


## *A Novel Nanobio Catalyst for Biofuels, SAXS*

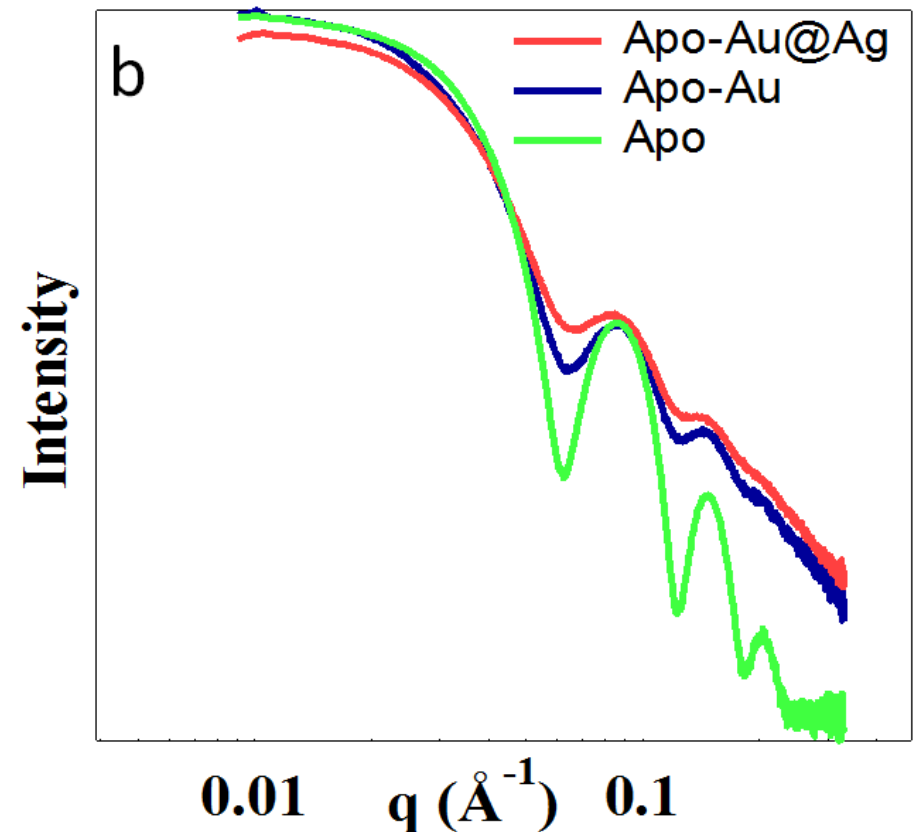
Synthesis of Au-core Ag-shell nanocatalyst  
5 nm fairly mono-dispersed within Apo ferritin



SAXS Calculated Data



SAXS Experimental

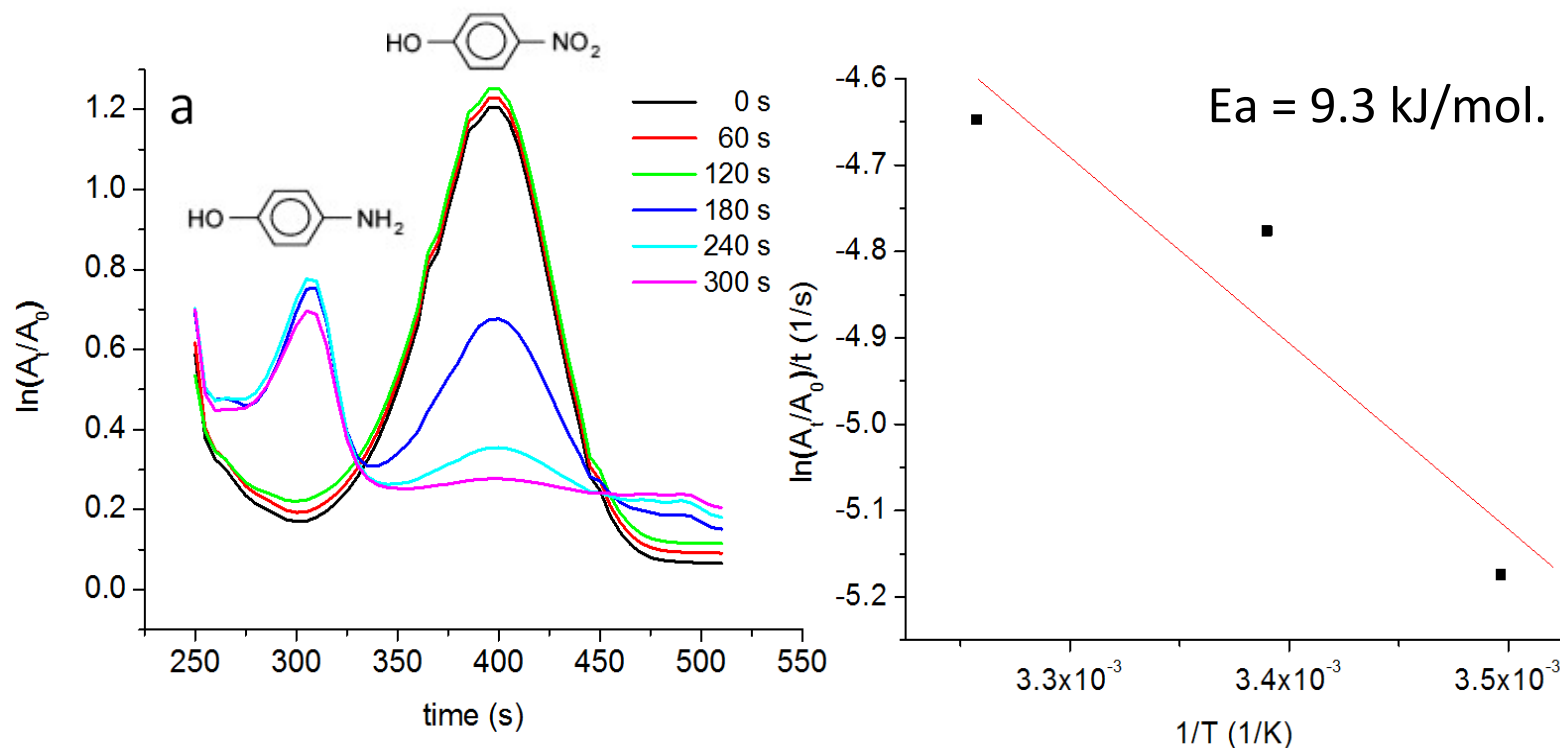


1. Particle forms in the protein cage.
2. Proteins keep their shape.

# Effect of Ligand-free Nanoparticle Catalyst

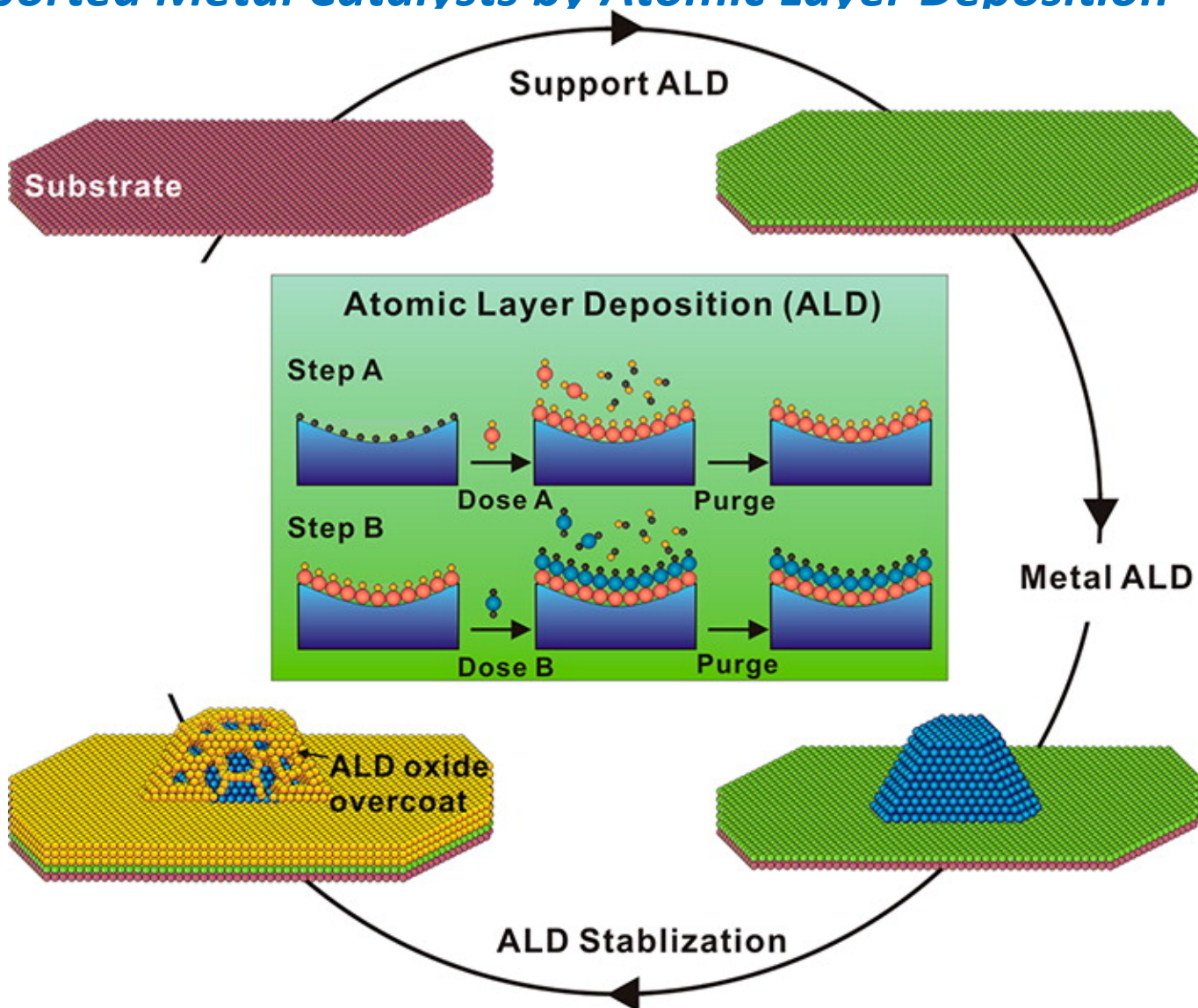
1. Reactant can pass through the protein shell
2. Lower activation energy than typical colloidal Au

Hydrogenation of 4-nitrophenol in water with  $\text{NaBH}_4$



Literatures: 38 kJ/mol (J Mol Catal a-Chem 2009, 298, 7-11), 28 kJ/mol (Au nanocages), 44 kJ/mol (Au nanoboxes), and 55 kJ/mol (partially hollow nanoboxes) (Nano Lett 2010, 10 (1), 30-35).

# Synthesis and Stabilization of Supported Metal Catalysts by Atomic Layer Deposition



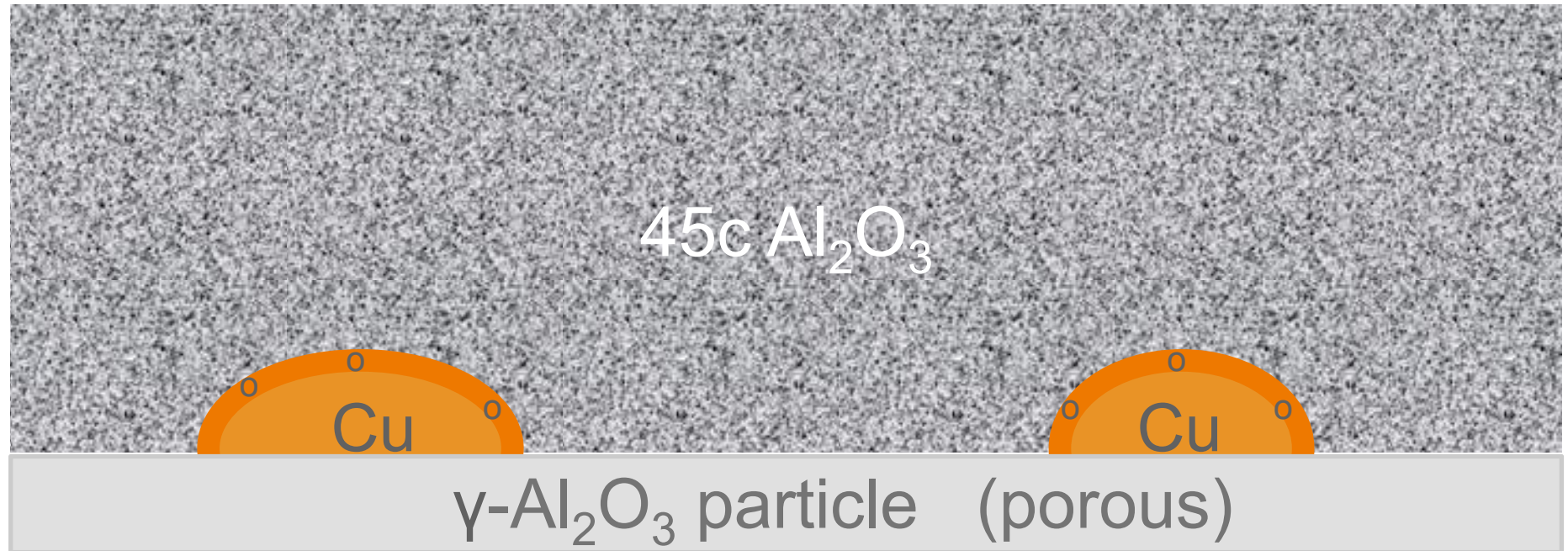
Lu, Junling; Elam, Jeffrey W.; Stair, Peter C.  
Accounts of Chemical Research (2013), 46(8), 1806-1815







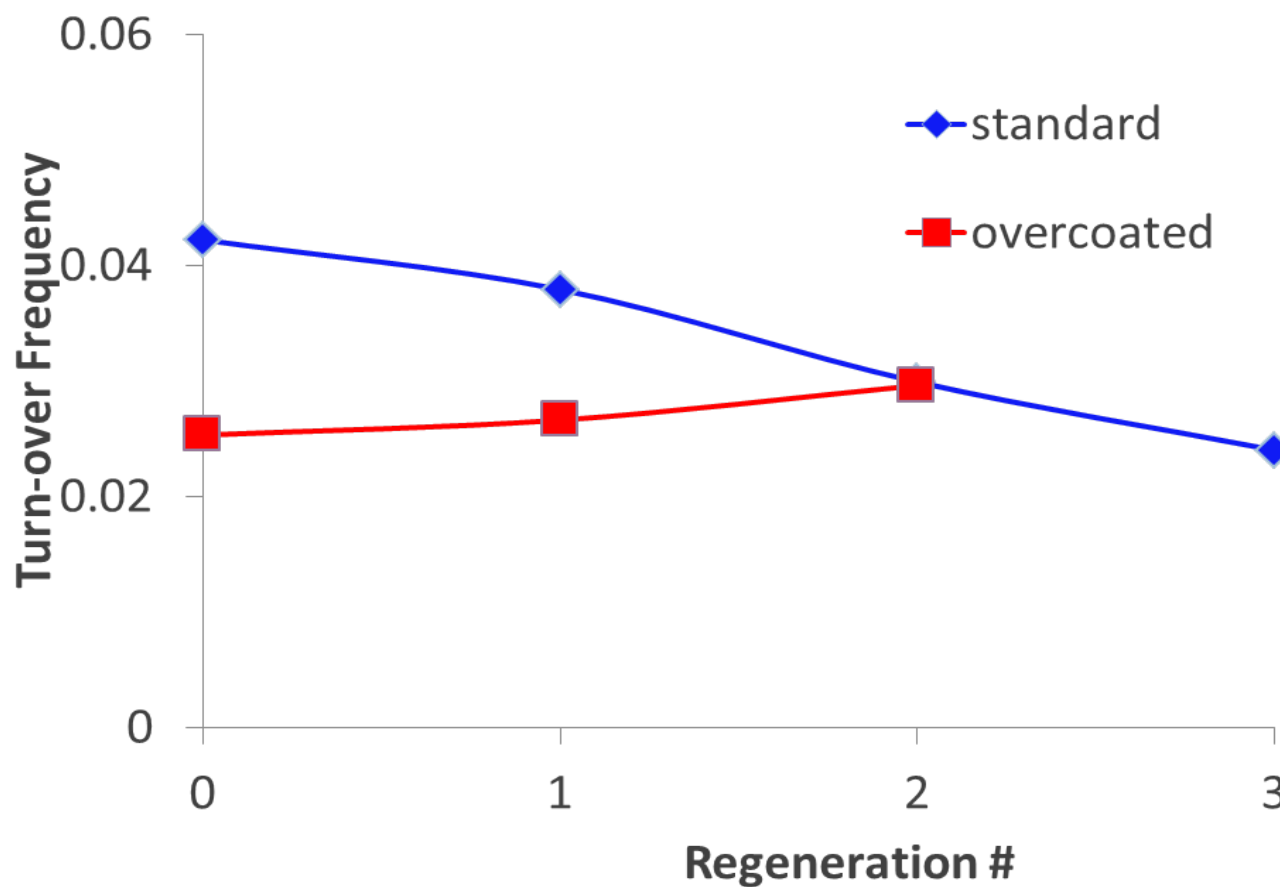
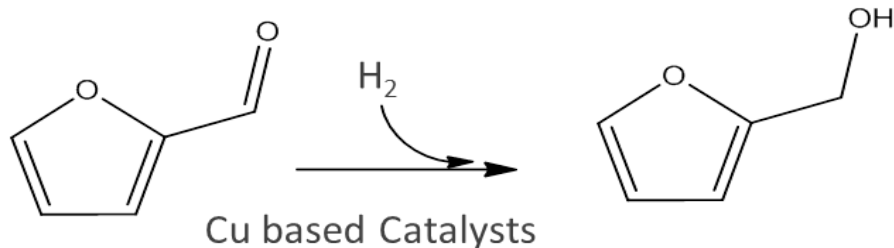
# 45ALD/Cu/ $\gamma$ -Al<sub>2</sub>O<sub>3</sub>



Brandon O'Neill, James Dumesic, UWM

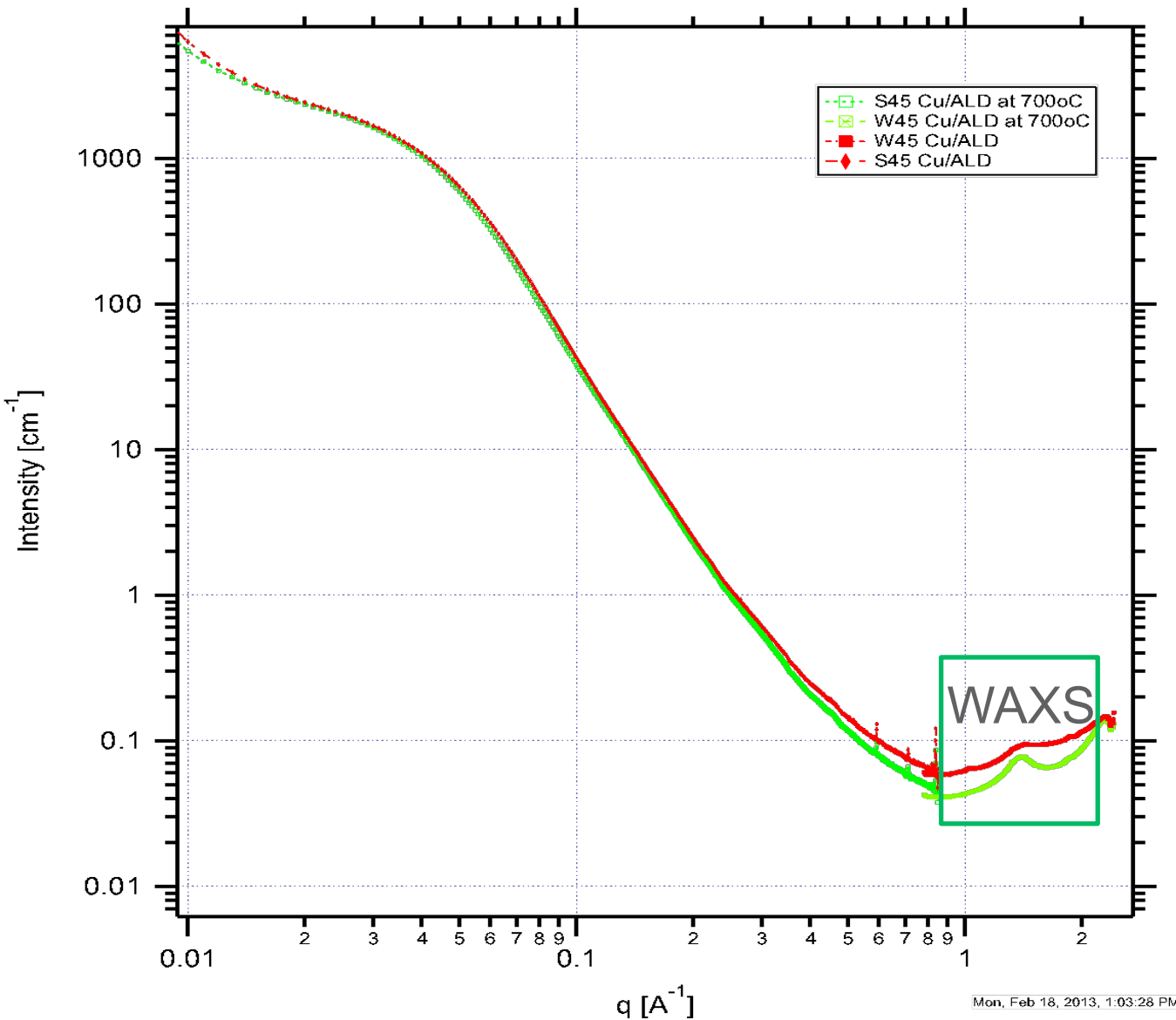


# Hydrogenation of Furfural



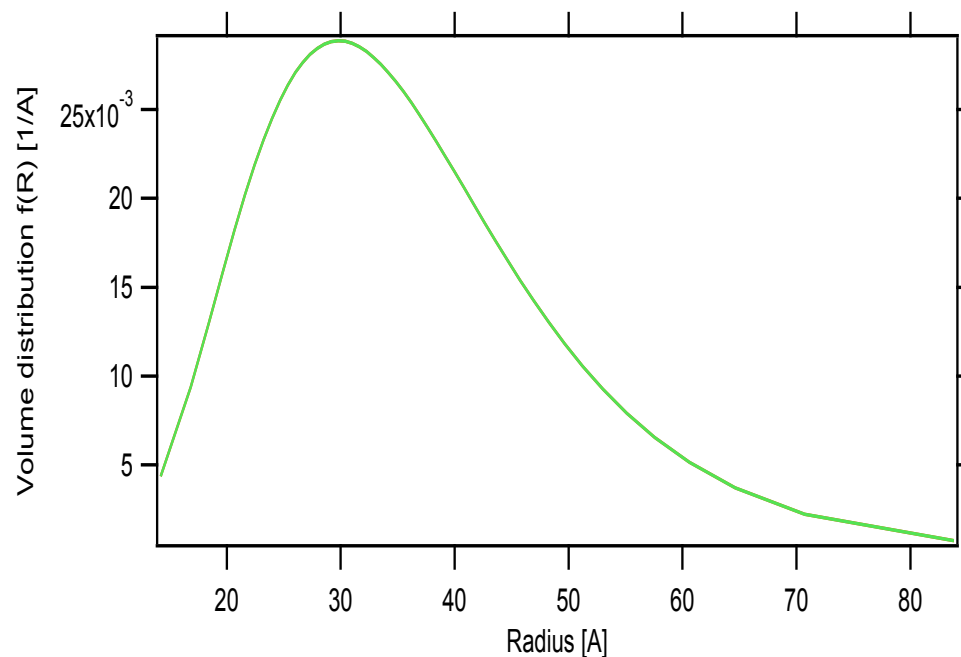
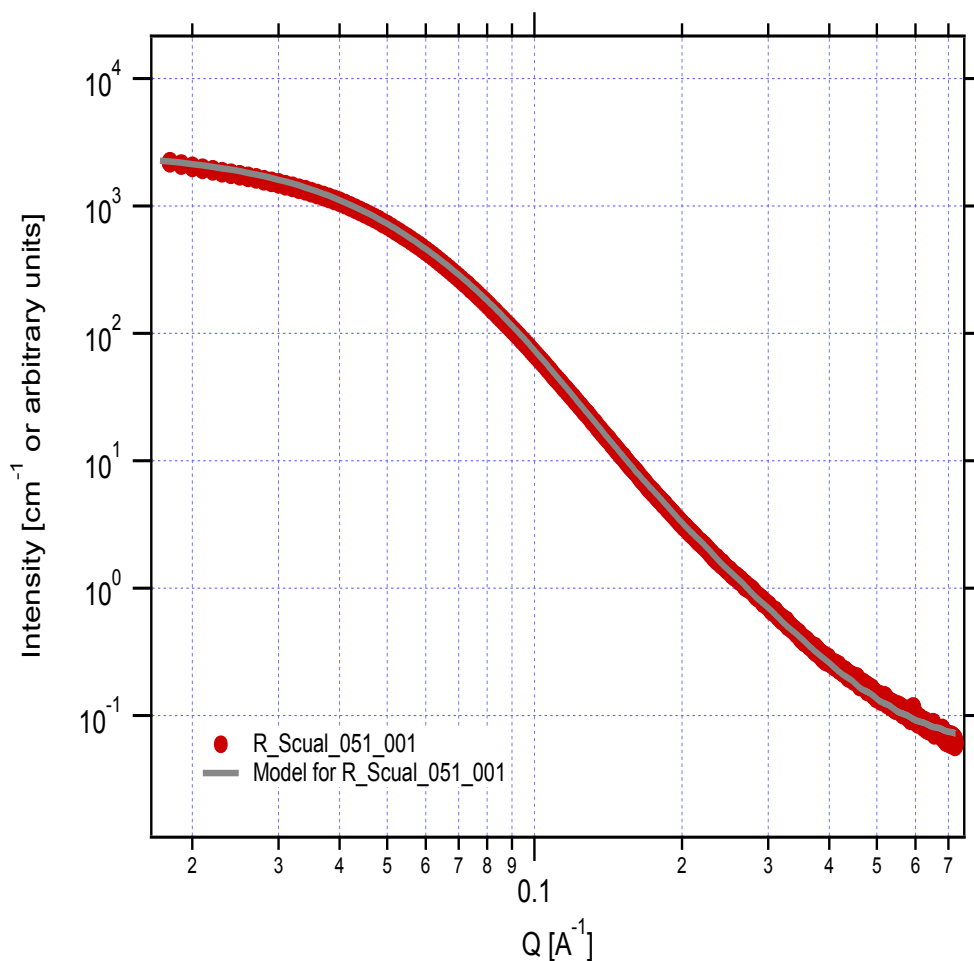
Brandon O'Neill, James Dumesic, UWM

# Pore from Crystallization of $\text{Al}_2\text{O}_3$



- The WAXS data show that after heating, the  $\text{Al}_2\text{O}_3$  changes from amorphous to crystallized.
- SAXS can measure the pore size from the difference of the samples.
- *Hard to find good background for the subtraction.*

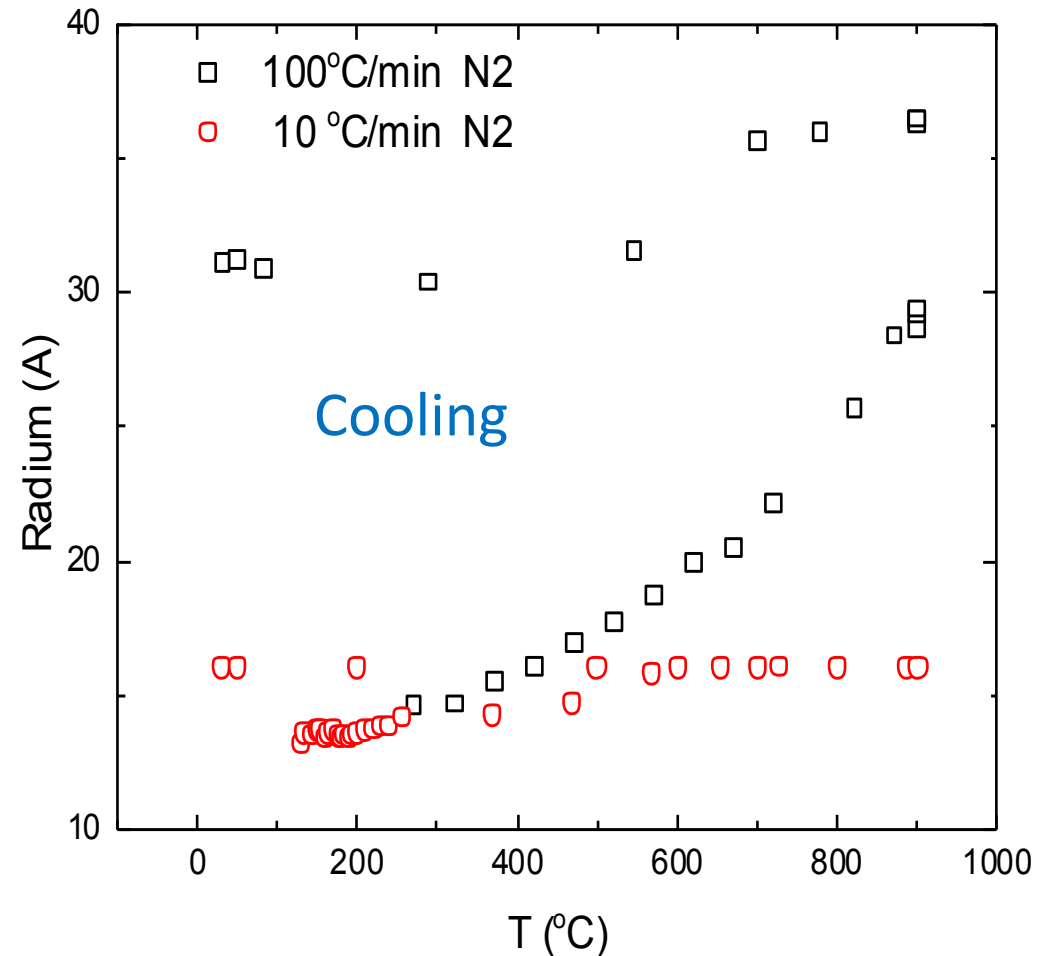
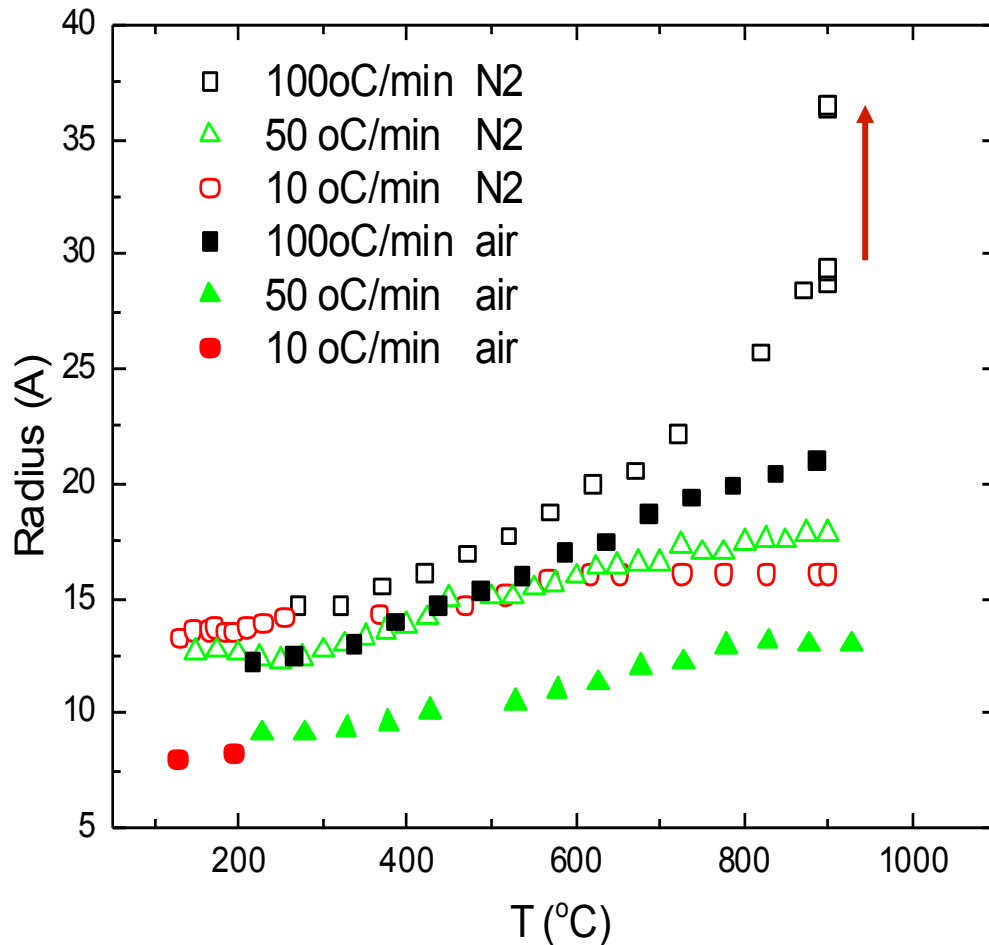
# Pore Size of $\gamma$ -Al<sub>2</sub>O<sub>3</sub> Support from SAXS



**The fitting shows that the average particle size is 6.7 nm, consistent with BJH data 7.1 nm.**



## Control of Thermal Pore Formation Followed by SAXS

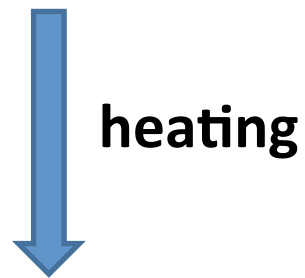
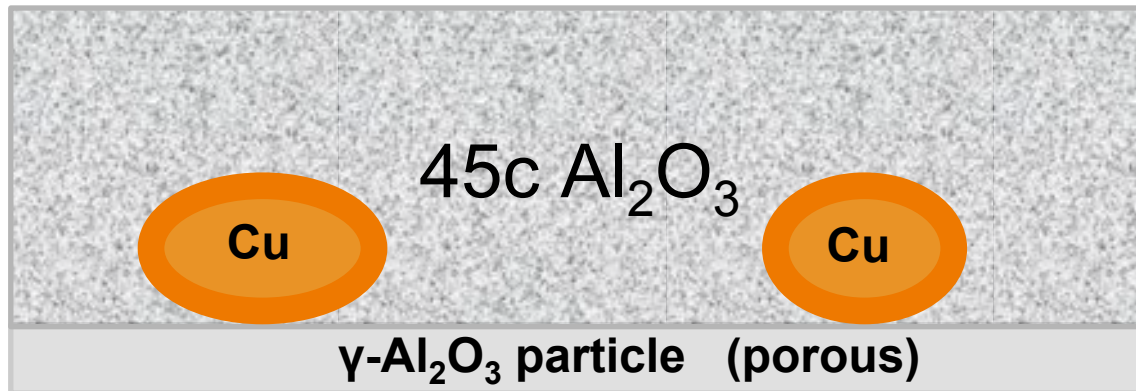


- The pore size increases as the temperature increases.
- With greater ramping rates, the larger pores form
- The pore is larger heated in the N<sub>2</sub> than in the air.
- During the cooling, the pore size can be controlled by the previous heating rate.

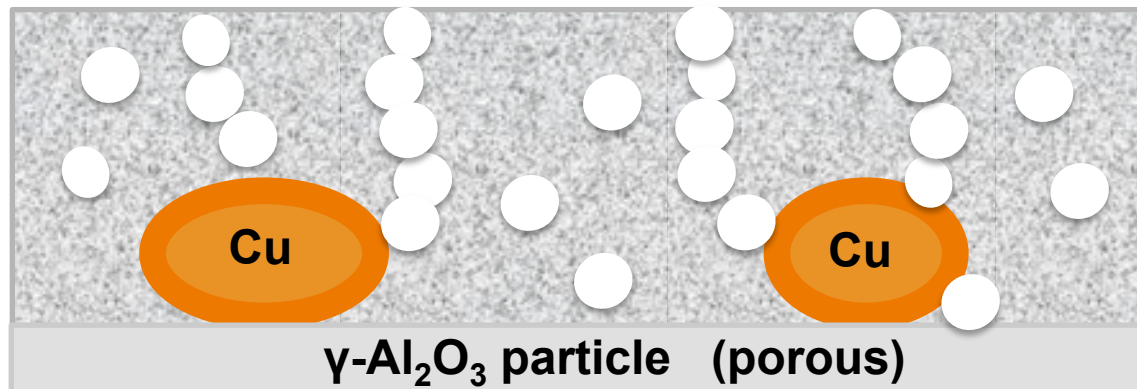


## *In situ SAXS of Calcination of ALD OverCoating*

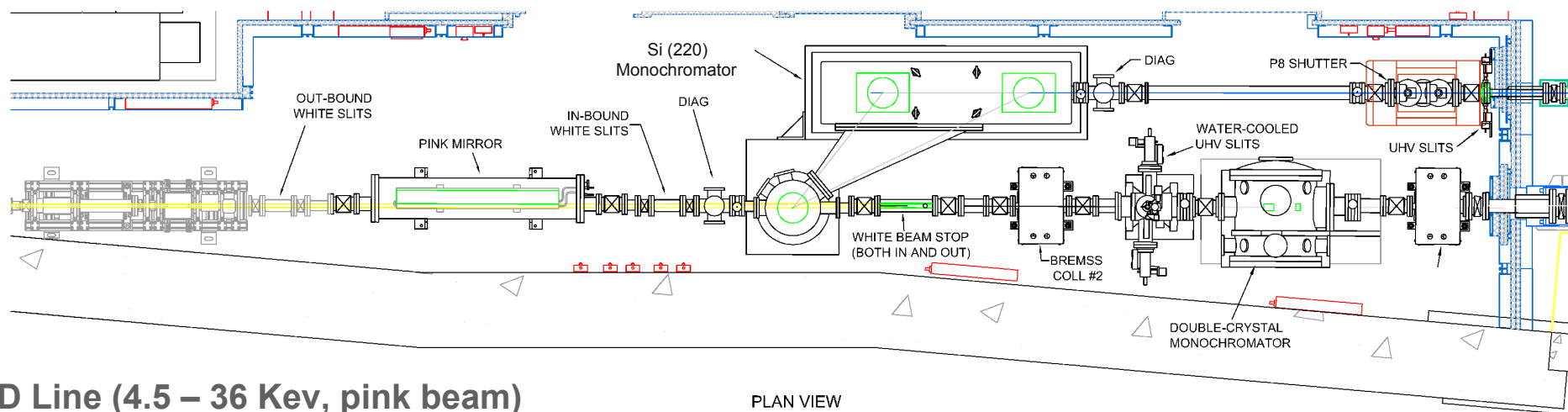
Cu particles over coated with  $\text{Al}_2\text{O}_3$  ALD



J. Elam and Saurabh Karwal (ANL) are doing a simulation of this pore forming process



# 12 - ID Upgrade to Two Beamlines with Canted Undulators



## ■ C/D Line (4.5 – 36 Kev, pink beam)

SAXS/WAXS/GISAXS/GIXAS - in situ, time resolved [12-ID-C]

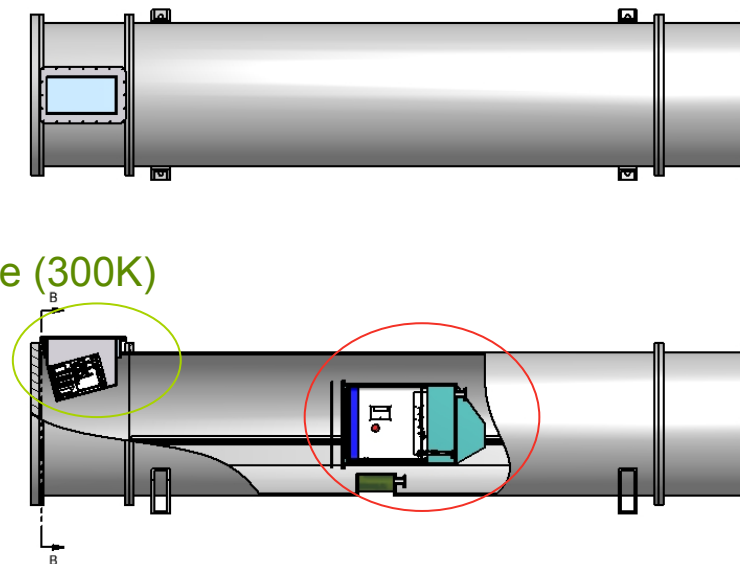
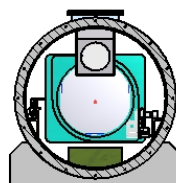
Surface Scattering – MOCVD, surface diffraction [12-ID-D]

## ■ B Line (7.4 – 13.9 Kev)

SAXS/WAXS/GISAXS - rapid adjustable Q [12-ID-B]

## ■ Detectors

APS/XOR Platinum mosaic CCD, **Pilatus 2M** and **wide angle (300K)**



# A Complete Catalysis in situ Study - Synthesis Steps, Reaction, and Re-activation

